

APPLICATION OF HOLOGRAPHIC INTERFEROMETRY TO
SUPERSONIC FLOW VISUALIZATION OF A REAR-FACING
STEP AND APPLICATION OF FAST FOURIER TRANSFORM
METHODS TO CURRENT DATA REDUCTION TECHNIQUES

Harland Wilber Jones

DUDLEY KNOX LIBRARY
NAVAL POSTGRADUATE SCHOOL
MONTEREY, CALIFORNIA 93940

NAVAL POSTGRADUATE SCHOOL

Monterey, California



THESIS

APPLICATION OF HOLOGRAPHIC INTERFEROMETRY TO
SUPERSONIC FLOW VISUALIZATION OF A REAR-FACING
STEP AND APPLICATION OF FAST FOURIER TRANSFORM
METHODS TO CURRENT DATA REDUCTION TECHNIQUES

by

Harland Wilber Jones, Jr.

Thesis Advisor:

D. J. Collins

March 1974

T160136

Approved for public release; distribution unlimited.

Application of Holographic Interferometry to
Supersonic Flow Visualization of a Rear-Facing
Step and Application of Fast Fourier Transform
Methods to Current Data Reduction Techniques

by

Harland Wilber Jones, Jr.
Lieutenant, United States Navy
B.S., United States Naval Academy, 1968

Submitted in partial fulfillment of the
requirements for the degree of

MASTER OF SCIENCE IN AERONAUTICAL ENGINEERING

from the

NAVAL POSTGRADUATE SCHOOL
March 1974

ABSTRACT

The successful application of holographic interferometry to the study of three-dimensional density fields around bodies in wind tunnel experiments has been reported in the literature along with the associated mathematical reduction processes for the basic interferometric equation.

The present report has extended the application of holography as a flow visualization technique by investigating Mach 2.8 flow over a rear-facing $1/8$ in. step. Two single-exposed holograms of the model and two double-exposed frozen fringe holographic interferograms of the flow were created.

Fast Fourier Transform (FFT) methods have been reported as significantly reducing computational time to obtain discrete and inverse discrete Fourier transforms. Two computer programs were designed to apply FFT methods to the Fourier transform approach to the basic interferometric equation. These programs were used to investigate an alternate way to calculate the value of the inside integral. Total agreement was not found, and further analysis as to the accuracy of each method is needed.

TABLE OF CONTENTS

| | | |
|-------|--|----|
| I. | INTRODUCTION..... | 9 |
| II. | INTRODUCTION TO HOLOGRAPHY..... | 10 |
| III. | INVESTIGATION OF A REAR-FACING STEP..... | 12 |
| IV. | EXPERIMENTAL MODEL..... | 13 |
| V. | DESCRIPTION OF APPARATUS..... | 14 |
| VI. | EXPERIMENTAL PROCEDURE..... | 15 |
| VII. | FILM AND DEVELOPMENT PROCEDURE..... | 16 |
| VIII. | RECONSTRUCTION TECHNIQUE, EQUIPMENT, AND RESULTS..... | 17 |
| IX. | CURRENT DATA REDUCTION TECHNIQUES..... | 19 |
| X. | APPLICATION OF THE FAST FOURIER TRANSFORM..... | 24 |
| XI. | RESULTS AND RECOMMENDATIONS FOR FFT APPLICATION..... | 28 |
| XII. | SUMMARY OF RESULTS..... | 30 |
| | FIGURES..... | 31 |
| | APPENDIX A: Detailed Experimental Procedures..... | 43 |
| | APPENDIX B: The Inside Integral Subsection Of Van Houten's Computer Program..... | 45 |
| | APPENDIX C: FFT Convolution Procedures: | |
| | 1. Computation Procedure For FFT Convolution Of Finite-Length Functions..... | 46 |
| | 2. Computation Procedure For FFT Convolution: Select-Savings Method..... | 47 |
| | 3. Computation Procedure For FFT Convolution: Overlap-Add Method..... | 48 |
| | APPENDIX D: SUBROUTINE CFFT2..... | 49 |
| | APPENDIX E: MODE1--Mode One Operation Of Van Houten's Computer Program With Some Modifications..... | 67 |

APPENDIX F: Alternate Programs Designed To Calculate The Value Of
The Inside Integral:

- 1. JONES1--Using Convolution Values Obtained Numerically.....78
- 2. JONES2--Using Convolution Values Obtained With FFT Methods.....80
- 3. Listing Of The Expanded Fringe Shift Information Values Supplied To Both JONES1 And JONES2.....83

APPENDIX G: Comparison Of JONES1 And JONES2 Values Of The Inside
Integral With Van Houten's Values Of The Inside
Integral.....85

REFERENCES.....86

INITIAL DISTRIBUTION LIST.....88

FORM DD 1473.....89

LIST OF FIGURES

| | |
|--|----|
| 1. Chapman-Korst Flow Model for Supersonic Base Flow..... | 31 |
| 2. Lip Shock..... | 32 |
| 3. The Experimental Model of a Rear-Facing Step..... | 33 |
| 4. Experimental Model..... | 34 |
| 5. Experimental Setup..... | 35 |
| 6. A View of the Left Side of the Experimental Setup Showing the Laser and the Optics System up to the Beam Splitter..... | 36 |
| 7. View of the Left Side of the Test Section, also Showing the Q-Switched Laser, the Beam Splitter, and Mirrors which Direct the Reference Beam over the Test Section..... | 36 |
| 8. A View of the Right Side of the Test Section..... | 37 |
| 9. A View of the Right Side of the Experimental Setup Showing the Holographic Plane and the Final Mirrors for the Reference and the Scene Beams..... | 37 |
| 10. Reconstruction Setup..... | 38 |
| 11. Photograph of the Projected Real Image of a Single-Exposed Hologram..... | 39 |
| 12. Photograph of the Projected Real Image of a Single-Exposed Hologram..... | 39 |
| 13. Photograph of the Projected Real Image of a Double-Exposed Hologram of a Rear-Facing 1/8 in. Step in Mach 2.8 Flow..... | 40 |
| 14. Photograph of the Projected Real Image of a Double-Exposed Hologram of a Rear-Facing 1/8 in. Step in Mach 2.8 Flow..... | 40 |
| 15. The Number of Operations Required to Compute the Discrete Fourier Transform by Direct Calculation Compared with Using the FFT Algorithm..... | 41 |
| 16. Optimum Value of N for FFT Convolution..... | 42 |

TABLE OF SYMBOLS

| Symbol | Meaning |
|--------------|---|
| DFT | Discrete Fourier transform |
| DR | Interval between frequency plane values, used as a weighting function for determining the convolution |
| $F(A)$ | Operator meaning "to take the discrete Fourier transform of 'A'" |
| $F^{-1}(A)$ | Operator meaning "to take the inverse discrete Fourier transform of 'A'" |
| FFT | Fast Fourier transform |
| IDFT | Inverse discrete Fourier transform |
| L | Length |
| M | Mach number |
| mW | Milliwatt |
| n, n_0 | Index of refraction, reference index of refraction |
| NP | Number of points of frequency plane values |
| Q | Number of frequency plane values in the finite sample |
| r | Radius |
| R | Radius of convolution vector |
| RMAX | Maximum radius of original finite frequency plane values |
| S_i | The i^{th} region of integration |
| dS_i | Distance along the i^{th} ray traversing the test section |
| t | Step size of rear-facing step |
| U | Local velocity |
| \AA | Angstrom degree, equal to 10^{-8} cm. |
| γ | Power of 2, i.e. 2^γ |
| $(C1 * C2)$ | "*" Operator meaning "C1 is convoluted with C2" |

| | |
|----------------------------------|---|
| $\frac{\partial(a)}{\partial b}$ | Operator meaning the "partial derivative of 'a' with respect to 'b'" |
| θ | Angular measurement in polar coordinates |
| ν | Coefficient of viscosity for fluid involved in the flow under consideration |
| φ | View angle |
| ρ_i | Known path length function; frequency plane values |
| ρ | Distance from origin in polar coordinates |
| ρ, ρ_0 | Density, reference density |

ACKNOWLEDGMENTS

The writer wishes to gratefully acknowledge Dr. D. J. Collins for his most valuable guidance and assistance throughout the course of this investigation; the technical staff of the Department of Aeronautics under R. Besel and T. Dunton, particularly N. Leckenby for his invaluable assistance in construction and operation of the experimental equipment and G. Middleton for his fabrication of the experimental model; Deborah Janov for her considerable effort in the final preparation and typing of this report; and my wife and family for their noble patience and encouragement.

I. INTRODUCTION

This thesis contains both an experimental section and a theoretical section. The experimental portion involved the construction of a modified Z-type Schlieren system to conduct holographic investigation of a rear-facing step in supersonic flow. The theoretical portion involved investigating current data reduction techniques for determining the three-dimensional distribution of a field by applying fast Fourier transform methods to solve the basic interferometric equation. Two original computer programs were devised in an attempt to reduce computer computational time required for interferometric data reduction.

II. INTRODUCTION TO HOLOGRAPHY

Holography is a three-dimensional photography-like process which involves the recording of both phase and amplitude information of light waves diffracted by an object illuminated with coherent light. Originally proposed by Gabor [1,2] in 1948, holography awaited the development of the laser around 1960 to become an explosive field of its own. The laser contributed a basically monochromatic, coherent light source. The property of coherence, or the capability of interference with itself, enables the recording of both phase and amplitude information.

Photography records the intensity of illumination, which is the time average of the square of the amplitude of the light field at any point. In holography, a coherent light beam is separated into a reference beam and an object (or scene) beam. The reference beam is directed to the holographic plane via an optics system while the object beam reaches the same point after being diffracted by a subject of interest. The emulsion on the holographic plate records the intensities of the illuminating beams and the interference between the two beams. The interference component contains the phase information which permits reconstruction of an image possessing full three-dimensionality and parallax properties. No attempt will be made to present the full mathematical and historical development of holography which is amply done in many excellent texts. [3]

Among its many engineering applications, holography is well suited for flow visualization. Recent successful applications of holography at the Naval Postgraduate School include the study of a free jet and the determination of the density field about a cone tilted in supersonic flow in a conventional wind tunnel. The use of double-pulsed holography is

especially helpful as a tool for measurement in high velocity flows near vibrating equipment such as free jets and blow-down wind tunnels. A Q-switch ruby laser is used as a high power energy source emitting a coherent light pulse on the order of several joules in an extremely small time span, on the order of twenty nanoseconds. Vibrations of the object or of the optical system components, which must remain stable within wave lengths of light during exposure of the hologram, are of negligible importance due to the very short duration of the exposure time.

A double-pulsed (or double-exposed) approach is advantageous in flow visualization. In the Mach-Zender interferometer, comparison of the reference and object beams are made at the same time. With holography it is possible to separate the simultaneous comparison in time. Two holograms, or exposures, are made on the same holographic plate without intermediate development. The first exposure is made with no flow and the second with flow. The individual holograms interfere with each other, creating an interferogram of the flow. Essentially, this interferogram contains only the differences in optical path lengths between the two exposures. Therefore, any imperfections in optical components, (which are identical for both exposures), are subtracted out, thereby eliminating the need for high quality optics [4].

Another method of taking finite fringe holograms is the double-exposure option of the dual hologram method, which involves using two holographic plates. One plate is used for each exposure. A dual hologram holder positions each plate in the same location for its exposure. The improvement comes from the versatility of almost an infinite set of reconstruction possibilities from one set of plates. A dual hologram holder has recently been constructed at the Naval Postgraduate School to demonstrate its application. This topic was the subject of AIAA Paper 73-210 [5].

III. INVESTIGATION OF A REAR-FACING STEP

Holographic investigation of a rear-facing step in supersonic flow was selected for two main reasons. First, extensive theoretical and experimental investigations of a rear-facing step in two-dimensional supersonic flow are available. This provides ample information for verifying results from this experiment. Secondly, previous experimental results do not completely agree with theoretical descriptions. A source of conflict is the lip shock's influence on the rest of the flow as it pertains to the reattachment point and to the tail shock. With this in mind, it was hoped to provide a hologram which could be used to accurately reproduce the flow field.

The classical flow model for supersonic base flow, (rear-facing step flow), was proposed by Chapman [6] in 1957 and independently by Korst [7] for turbulent flow, and is commonly known as the Chapman-Korst flow model. Refer to Figure 1 for a sketch of the Chapman-Korst flow model. Roache [8] presented a literature search and a review of discrepancies with this model in his doctoral thesis for the University of Michigan in 1968. The main, unresolved discrepancies in the Chapman-Korst flow model were: that the experimental pressure at recompression was not equal to the theoretical pressure of Region Four (see Fig. 1); and that the isentropic turn from Regions One to Two (see Fig. 1) and the constant pressure assumptions were invalidated by the presence of the lip shock (see Fig. 2) at higher Mach numbers. [9]

The opportunity to provide some accurate data on these unresolved areas of interest appeared to be a worthwhile application of holography.

IV. EXPERIMENTAL MODEL

The actual rear-facing step model used was limited in size, with the maximum step size being one-eighth inch. Due to the small step size, the boundary layer thickness (δ) was compared with the step size (t) to determine if distortions from the boundary layer would invalidate experimental results. From Schlichting [10], the applicable equations are: $\delta = 5 (\nu L / U)^{\frac{1}{2}}$ for laminar flow; and $\delta / L = .37 (U L / \nu)^{-1/5}$ for the boundary layer thickness at the trailing edge of a flat plate at zero incidence in parallel turbulent flow. The δ / t ratio results were .0538 for laminar flow and .218 for turbulent flow. It was felt that the actual flow situation was laminar and that this step size would still offer meaningful results.

A photograph of the model is included as Figure 3. Refer to Figure 4 for a sketch showing the dimensions of the model.

V. DESCRIPTION OF APPARATUS

Figure 5 shows a complete sketch of the experimental setup. A modified Z-type Schlieren system, it was constructed specifically for this thesis. A description of the integrated setup will be followed by listing of important supportive equipment.

A high energy pulse was discharged from a Q-switch ruby laser and passed through a diffusing lens to a collimating mirror in order to expand the light beam to sufficiently illuminate the test section. The collimated beam reflected off a flat mirror towards the test section. Just prior to the test section, the beam was divided by a beam splitter mounted on a tripod. The object (scene) beam transmitted through the beam splitter, through the test section, and reflected off another flat mirror towards a converging mirror. The object beam was then reflected towards the holographic plane which was positioned in the diverging part of the beam where the test object was in focus. The part of the collimated beam reflected by the beam splitter, the reference beam, reflected off three flat mirrors and also illuminated the holographic plane.

Other equipment included an air supply for the tunnel provided by an air compressor; a power supply and cooling system for the laser; a 15 mW continuous wave Helium-Neon laser used for alignment of the Q-switched ruby laser with the optics system; an autocollimator for internal alignment of the Q-switch laser; a movable platform for the laser so it can be elevated to the proper height for the optics system; a table for the hologram holder; and mountings and supports for all optic components. Figures 6-9 are pictures showing the experimental setup from four different views.

Safety equipment included eye protectors and sound attenuators.

VI. EXPERIMENTAL PROCEDURE

Appendix A contains a detailed description of the entire experimental procedure from alignment of system components to exposure of various types of holograms.

There are two holographic methods that can be applied to flow visualization in wind tunnels. The first method is commonly referred to as the real fringe method, and the second as the frozen fringe or double-exposed method.

Real fringe methods require exposure of the holographic plate with no flow in the wind tunnel and either development of the hologram in place or precise repositioning of the developed plate. As flow is increased in the wind tunnel, an evolution of real fringe patterns could be observed through the hologram. This method was not used in this experiment due to the unavailability of in-place developing equipment or a dual-hologram holder.

Double-exposed or frozen fringe methods require two exposures of the same holographic plate. The first exposure is taken with no flow in the wind tunnel, and the second with flow. The interference between the two exposures results in a double-pulsed (exposed) interferogram. In this experiment both exposures were made on the same plate with the second exposure occurring while Mach 2.8 flow existed in the test section.

VII. FILM AND DEVELOPMENT PROCEDURE

There are essentially two sources of holographic films: Eastman Kodak Company and Agfa-Gevaert. Agfa-Gevaert films were used exclusively in this experiment because their 75 series film is designed for maximum sensitivity around the emission spectrum of ruby lasers (6943 Å). Due to the short duration of the exposure time of the Q-switch ruby laser, about 10-20 nanoseconds, 10E75 film was used because 8E75 film turned out to be too slow in recording information.

Development of holograms can include various features such as bleaching, prehardening, or varying development time. The various alternatives are examined in Ref. 11. For this experiment the following development procedure was used:

1. Five minutes in Kodak D-19 Developer
2. Thirty seconds in an acetic acid stop bath of standard dilution.
3. Five minutes in a standard fixer.
4. Five minutes of washing followed by immersion in a wetting agent (Kodak Photoflo) prior to drying.

VIII. RECONSTRUCTION TECHNIQUE, EQUIPMENT, AND RESULTS

A 15 mW continuous wave Helium-Neon laser, previously used for alignment, was the coherent light source used for reconstruction. A collimating lens was attached to this laser in order to expand the reconstruction beam to approximately two inches. Other reconstruction equipment included a hologram holder, type 52P Polaroid film, a graphic view camera, a tripod, and a black drape.

The two-inch diameter collimated beam incident to the hologram created two images. Whether projected images are real or virtual is discussed in Chapter 3 of Ref. 3 for the various combinations of converging, diverging, and collimated reference and scene beams. In this experiment, approximate symmetry about the vertical axis of the holographic plate was attempted. This resulted in the real image being projected as a converging wave front and in the virtual image being projected as a diverging wave front.

In order to focus the real image, the lens was removed from a camera and the image was projected on the ground glass backing of the camera. Pictures of these projections were taken at exposure times which varied with the intensity of the real image beam. Normal exposure times were approximately one second.

Figure 10 is a sketch of the reconstruction setup and Figures 11-14 are examples of photographs of the projections of the real image of holograms taken with this experimental setup.

Figures 13 and 14 represent the final experimental attempts to create a frozen fringe hologram of sufficient quality to warrant data reduction. The edges of the experimental model show that both holograms are slightly out of focus. These holograms were, however, sufficient to demonstrate

the applicability of holography to flow visualization of a rear-facing step in supersonic flow. Additionally, the shadowgraph resulting on the developed plate showed the basic features of the Chapman-Korst flow model. Sufficient information was not obtained to analyze any of previously mentioned discrepancies of that model.

The remaining effort of this thesis focused on the possibilities of improving current data reduction methods.

IX. CURRENT DATA REDUCTION TECHNIQUES

There are currently several approaches for reducing an asymmetric density field. One method involves a series expansion of a complete set of orthogonal polynomials which are invariant to a rotation of coordinates [12]. Matulka, [13] used this method and created a computer program which took approximately two hours of computer time to reduce the data for the asymmetric case.

A second approach uses Fourier transform techniques suggested by Rowley [14] and further developed by Junginger and van Haeringen [15]. This approach is thoroughly discussed by Sweeney [16] in his doctoral thesis for the University of Michigan in 1972.

Closely following Sweeney's development and nomenclature, the fundamental integral equation to be solved in three-dimensional interferometry is

$$\int_{S_i} f(x,y,z) dS_i = \phi_i \quad (9-1)$$

where $f(x,y,z)=n(x,y,z)-n_0$; $f(x,y,z)$ is the refractive index relative to a known value n_0 , S_i is the distance along the i^{th} ray traversing the test section, ϕ_i is the known path length function, and the integral is evaluated between boundaries imposed by experimental configuration or by prior knowledge regarding $f(x,y,z)$. The objective is to reconstruct a real scalar function, the relative refractive index field, from the scalar values of line integrals through the field. When the gradient of the refractive index variation is small enough to produce negligible ray curvature, eqn. (9-1) alone is the basic interferometric equation to be solved. The line integrals are then evaluated along straight, not curved, lines.

The presentation of the problem is simplified by the suppression of one of the dimensions. Solutions for the two-dimensional case can be layered to reproduce the three-dimensional distribution, thereby permitting simplification without loss of information.

The use of polar coordinates on the two-dimensional equivalent of eqn. (9-1) yields

$$\int f(x,y) dS = \varphi(\rho, \theta) \quad (9-2)$$

where ρ varies to cover the domain of $f(x,y)$ and θ varies between $\pm \pi/2$. Eqn. (9-2) then becomes the fundamental integral equation to be solved.

If the refractive index field is radially symmetric or if it is independent of one of the coordinates, then the solution of eqn. (9-2) is known and has been extensively used in interferometric studies. For $f(x,y)=f(y)$ only, eqn. (9-2) becomes

$$\varphi(y) = \int_{-L/2}^{L/2} n(y) dx = L n(y) \quad (9-3)$$

and the solution is $n(y) = \varphi(y) L$.

For the radially symmetric case, only one field of view is necessary and eqn. (9-2) becomes

$$\varphi(x) = 2 \int_{r=x}^{\infty} f(r) dy = 2 \int_x^{\infty} \frac{f(r) dr}{(r^2 - x^2)^{\frac{1}{2}}} \quad (9-4)$$

which is a form of Abel's integral equation.

The solution of eqn. (9-4) may be obtained by converting the integral into a convolution integral by using appropriate transformations. The solution, $f(r)$, then becomes

$$f(r) = \frac{-1}{\pi} \int_r^{\infty} (x^2 - r^2)^{\frac{1}{2}} \frac{d}{dx} \left[\frac{\partial \varphi}{\partial x} \frac{1}{x} \right] dx \quad (9-5)$$

Sweeney uses the definitions of Fourier transforms, a few fundamental transform pairs, the procedure for inverting the Fourier transformed

equivalent of eqn. (9-2) as outlined by Junginger and van Haeringen [15], and an introduction of polar coordinates to the transformed equation to yield

$$f(r,\varphi) = \frac{1}{2\pi^2} \int_{-\pi/2}^{\pi/2} d\theta \left[\frac{\partial \varphi(z,\theta)}{\partial z} * \frac{1}{z} \right] \quad (9-6)$$

where "*" denotes the convolution. Expanding the convolution integral and replacing z with $r \sin(\varphi-\theta)$, the final result for $f(r,\varphi)$ is:

$$f(r,\varphi) = \frac{1}{2\pi^2} \int_{-\pi/2}^{\pi/2} d\theta \int_{-\infty}^{+\infty} \frac{\partial \varphi(\rho,\theta)}{r \sin(\varphi-\theta)} \frac{1}{-\rho} \partial \rho \quad (9-7)$$

This is the basic relationship between the pathlength function and the refractive index field.

Referring to eqn. (9-6), the integral over θ is a linear summation of the contributions for each direction of view. The contribution from each value of θ is equal to the convolution of the derivative of the path length function and, $(1/z)$ with $(1/z)$ evaluated at $z = r \sin(\varphi-\theta)$

When $\rho = r \sin(\varphi-\theta)$, the integrand of eqn. (9-7) becomes singular. This presents no problem since the contributions to the integral near the origin tend to cancel for an odd function (like $1/z$). Thus the integral remains finite.

The integration over ρ in eqn. (9-7) is a Hilbert transform of $\varphi(\rho,\theta)$ and the properties of Hilbert transforms along with the use of discrete data, guarantee the boundness of eqn. (9-7). Both this form of the integration over ρ and Van Houten's [17] modification to it will be called the inside integral in the next section.

A finite number of values of the frequency plane must be determined. One method for their determination uses linear interpolation from adjacent radial lines of a superimposed grid system. Success of this method depends on the accuracy of the interpolation. If the pathlength data is

taken for a sufficiently large number of angular orientations, linear interpolation may be used.

These linearly interpolated frequency plane values ($\varphi(\rho, \theta)$) must be convoluted with $1/z$, i.e.

$$[\varphi(\rho, \theta) * 1/z] \quad (9-8)$$

with "*" meaning convolution.

Using the following notation of F for obtaining the discrete Fourier transform (DFT) and F^{-1} for obtaining the inverse DFT or IDFT, the remaining steps required to perform the integration over ρ are summarized as follows:

The DFT of the convolution is obtained

$$F[\varphi(\rho, \theta) * 1/z] \quad (9-9)$$

followed by the differentiation of this function

$$d(F[\varphi(\rho, \theta) * 1/z]) \quad (9-10)$$

Finally the value for the integration over ρ is obtained by taking the IDFT of the preceeding function.

$$F^{-1} [d(F[\varphi(\rho, \theta) * 1/z])] \quad (9-11)$$

Van Houten [17] used the linear interpolation approach to obtain the frequency plane values by a computer program designed to calculate the three-dimensional density field from data obtained from holographic interferometry. The frequency plane values for the density field are represented by expanded fringe shift information calculated from the fringe number of specific points on the interferogram. Van Houten modified eqn. (9-7), the basic interferometric equation to the following:

$$f(x_o, y_o) = \frac{-1}{2\pi^2} \int_0^\pi \left[\int_0^{3RMAX} \frac{g(\rho_o + \rho, \varphi) + g(\rho_o - \rho, \varphi) - 2g(\rho_o, \varphi)}{2} d\rho \right. \\ \left. + \frac{2g(\rho_o, \rho)}{3RMAX} \right] d\varphi \quad (9-12)$$

with $g(\rho, \varphi)$ being the expanded fringe shift information and the integral inside the brackets referred to as the inside integral instead of the integration over ρ .

Van Houten's computer program uses Cote's sixth order method [18] for integrating the first term of the inside integral. He applied a correcting term for the contribution of the integral from 3RMAX to infinity. The sum of these two terms is called the inside integral. If NP is the number of data points for each view, and if K is the number of views, the inside integral must be evaluated $(NP \cdot K)$ times with Van Houten's computer program. Additionally, for each of the NP^2 grid intersections, K interpolations for $G(\rho_o, \varphi_k)$ are required. The subsection of Van Houten's computer program which calculates the value of the inside integral is included in Appendix B. The next section will investigate alternatives for this part of Van Houten's computer program.

X. APPLICATION OF THE FAST FOURIER TRANSFORM

Fast Fourier transform (FFT) methods are simply a more efficient means of obtaining the discrete Fourier transform (DFT). Their increased efficiency is due to the significant reduction in the number of complex mathematical operations required. For a function of N points, normal calculation of the DFT requires nearly N^2 operations while the FFT radix-2 method reduces this to $(N/2) \log_2(N)$ complex multiplications, $(N/2) \log_2(N)$ complex additions, and $(N/2) \log_2(N)$ complex subtractions. As can be seen from Figure 15, for $N=1024$, this results in a computational savings of more than 200 to 1. [19] Higher radix FFT methods further reduce the number of operations required.

Operations usually associated with FFT applications include: (1) computing a spectrogram; (2) computing the convolution of two time series; and (3) computing the correlation of two time series. The second of these operations has been shown to have direct application to the calculation of the value of the inside integral for determining the three-dimensional density field. Reference 20 gives a thorough discussion of the FFT and the required steps for convolution and correlation. These detailed procedures for computing the convolution are included in Appendix C for the following combination of functions: (1) two finite length functions; (2) a finite and an infinite length function using the select-savings method; and (3) a finite and an infinite length function using the overlap-add method.

Two original Fortran programs were devised to apply FFT methods to the calculation of the values of the inside integral. Specifically, alternatives to Mode One operation of Van Houten's computer program for the

asymmetric Gaussian case of $f(z) = (1-y^2) \exp(-2x^2)$ for 65 points from $-1.5 \leq R \leq 1.5$ were investigated. Mode One operation of Van Houten's program requires refractive index information supplied by SUBROUTINE INPUT. Using a finite sample of 65 points with an interval between samples of .046875, Van Houten's program required 1.3388 seconds of computer time just to calculate the value of the inside integral. This time was obtained by using computer library subroutines SETIME and GETIME placed just prior to and immediately after the subsection of Van Houten's computer program which calculates the value of the inside integral.

Van Houten's program also uses a SUBROUTINE COEFF to calculate coefficients used in various parts of the program. MODE1, a modification of Van Houten's program which eliminated the need for SUBROUTINE COEFF by returning its calculations to the main program, is included in Appendix D. This modification includes the essentials of Van Houten's thesis with the following corrections: $C1 = .292857$ instead of .2292857; several divisions by 59.296 were corrected to 57.296; and all plotting directions were deleted due to the storage space limitation of the IBM 360 on-line time sharing capability. This modification followed the work done by Everett [21].

Both FFT method programs used a finite sample of the expanded fringe shift information obtained from Van Houten's computer program. His method for obtaining these frequency plane values followed the linear interpolation approach as described by Sweeney. Sixty-five finite sample points were obtained and they had to be convoluted with the infinite function $1/z$. JONES1 numerically convoluted these functions while JONES2 used the FFT select-savings method to obtain the convolution. Once the convolution was obtained, both programs followed the procedures described in the preceding section, except that FFT methods were used to obtain all

DFT's and IDFT's. The two separate approaches for calculating the convolution served as an internal check that the correct convolution was being obtained. The complete programs are included in Appendix F. along with a listing of the expanded fringe shift information obtained from Van Houten's program and used as frequency plane values for both programs.

The numerical methods used in JONES1 required multiplying the final result by the appropriate weight function, the interval between sampled points of the expanded fringe shift information. JONES2 used the FFT select-savings method to calculate the convolution. The dimension of the $1/R$ vector was chosen to be 512 following Brigham's [20] recommendation as the optimal choice for values of Q between 50 and 99. His table of recommendations for the size of arrays needed for FFT convolution is included in Figure 16. The sample interval for both of these FFT programs was selected to agree with the interval used in Van Houten's program, namely .046875. For $N = 512$, and DR being defined as $2R_{MAX}/N$, an R of 12.0 was required. Using FFT methods to obtain the Fourier coefficients of the convolution also required a weighting function. In the complex multiplication of the normalized Fourier coefficients of the expanded fringe shift information and the $1/R$ vector, the resulting Fourier coefficients incorporated an extra division by N . Instead of a weighting function of DR then, $2R$ was chosen as the appropriate weighting function. When the IDFT of the Fourier coefficients was obtained, the values of the convolution by this FFT method were in exact agreement with the convolution obtained by numerical methods.

The differentiation technique used in JONES1 and JONES2 required an increment between steps of differentiation that was equal to the sample data interval. Thus, the same DR was used for this process.

All FFT calculations in both programs utilized SUBROUTINE CFFT2, an algorithm for computing the mixed radix fast Fourier transform [22]. The complete single precision version of CFFT2 is included in Appendix E. Chosen for its versatility, it contains a detailed and straight-forward usage description at the beginning of the subroutine. Several known Fourier transform pairs were investigated to ensure that CFFT2 was being used correctly. Correct DFT's and IDFT's were easily obtained.

As was previously mentioned, FFT methods involve complex mathematical operations. When using only real functions, as was the case with the expanded fringe shift samples and the $1/z$ function, the frequency plane values could be placed in the real coefficient array of CFFT2 and the other function could be placed in the imaginary coefficient array of the same call to CFFT2. This would result in the significant reduction of time and storage space required to calculate DFT's and IDFT's. This increased efficiency was not utilized in either JONES1 or in JONES2. Instead, both programs are quite inefficient, with redundant storage used for recording and checking each step in the entire process of calculating the value of the inside integral. If one only desired a print-out of the inside integral values, these programs could easily be reduced to four matrices, and possibly to two matrices since both functions were real in this case. Both programs, designed as possible alternatives for Van Houten's subsection that calculated the value of the inside integral, were only written to replace inside integral calculations for Mode One operation. Hence, in addition to condensing these programs into efficient packages, investigation of all other modes of operation is required before a complete integration of FFT methods into Van Houten's program can be achieved.

XI. RESULTS AND RECOMMENDATIONS FOR FFT APPLICATION

The computer time required for just the calculation of the inside integral subsection of Van Houten's program for Mode One operation of the asymmetric Gaussian case took 1.3388 seconds. Although the increased efficiency of FFT methods are significant for large values of N , it was not known if FFT methods would reduce computational time required in this case where N was only 64 sample intervals. Nevertheless, if time had permitted integration of a condensed and efficient form of either JONES1 or JONES2 into Van Houten's program, it was felt that some reduction in computation time would have been achieved.

Both approaches to obtain the convolution, JONES1 using numerical methods and JONES2 using FFT methods, produced convolution values in exact agreement with each other and inside integral values within .002 per cent of each other. A listing of these results side by side to the inside integral values obtained from Van Houten's program is included in Appendix G. There was general agreement between the values of the inside integral as calculated by Van Houten's program compared with those obtained by FFT methods. Near a value of R equal to $\pm .8$ the apparently significant percentage difference between the two methods was misleading since the magnitudes involved were small. However, for values of R near the discontinuity in the density, there was significant disagreement in the values of the inside integral. Further analysis as to the accuracy of the methods involved is required to resolve this problem.

Shifting the expanded fringe shift information from the middle of its array to the beginning of an array whose remaining points were filled with zeros, as suggested by the select-savings method, resulted in the

inside integral values corresponding to the $-1.5 \leq R \leq 1.5$ interval being stored in the output array beginning with the $(N/2 + 1)$ position. In this case, the appropriate values of the inside integral were stored from the 257th through the 321st positions of the output vector. According to the select-savings method (refer to Appendix C.2), the first "Q-2" points of the output vector are meaningless. Q is defined as the number of frequency plane samples used in the calculation of the convolution.

XII. SUMMARY OF RESULTS

An experimental setup was designed and constructed to conduct holographic investigation of a rear-facing step in supersonic flow. Although the double-exposed (frozen) holograms produced did not warrant further analysis of discrepancies of the Chapman-Korst flow model, they were of sufficient quality to demonstrate an application of holography to rear-facing step flow visualization near vibrating equipment such as the supersonic blowdown wind tunnel.

Theoretical investigations of current data reduction techniques for determining the three-dimensional density field from interferometric data led to investigation of the applicability of fast Fourier transform methods to reduce computational time required for determining the inside integration over ρ in the basic interferometric equation. Two programs were devised which calculated the value of the inside integral using FFT methods. Although the convolution was obtained differently for each program, numerically in JONES1 and with FFT's for JONES2, the convolution's were identical. Comparison of these values with those obtained from Van Houten's program lacked close agreement for the $\pm (1.07 - 1.31)$ intervals for R . The difference between these methods requires further analysis as to the accuracy of the methods. Further analysis is also needed to efficiently reduce JONES 1 and JONES2 and to integrate the programs into Van Houten's program for all of its modes of operation.

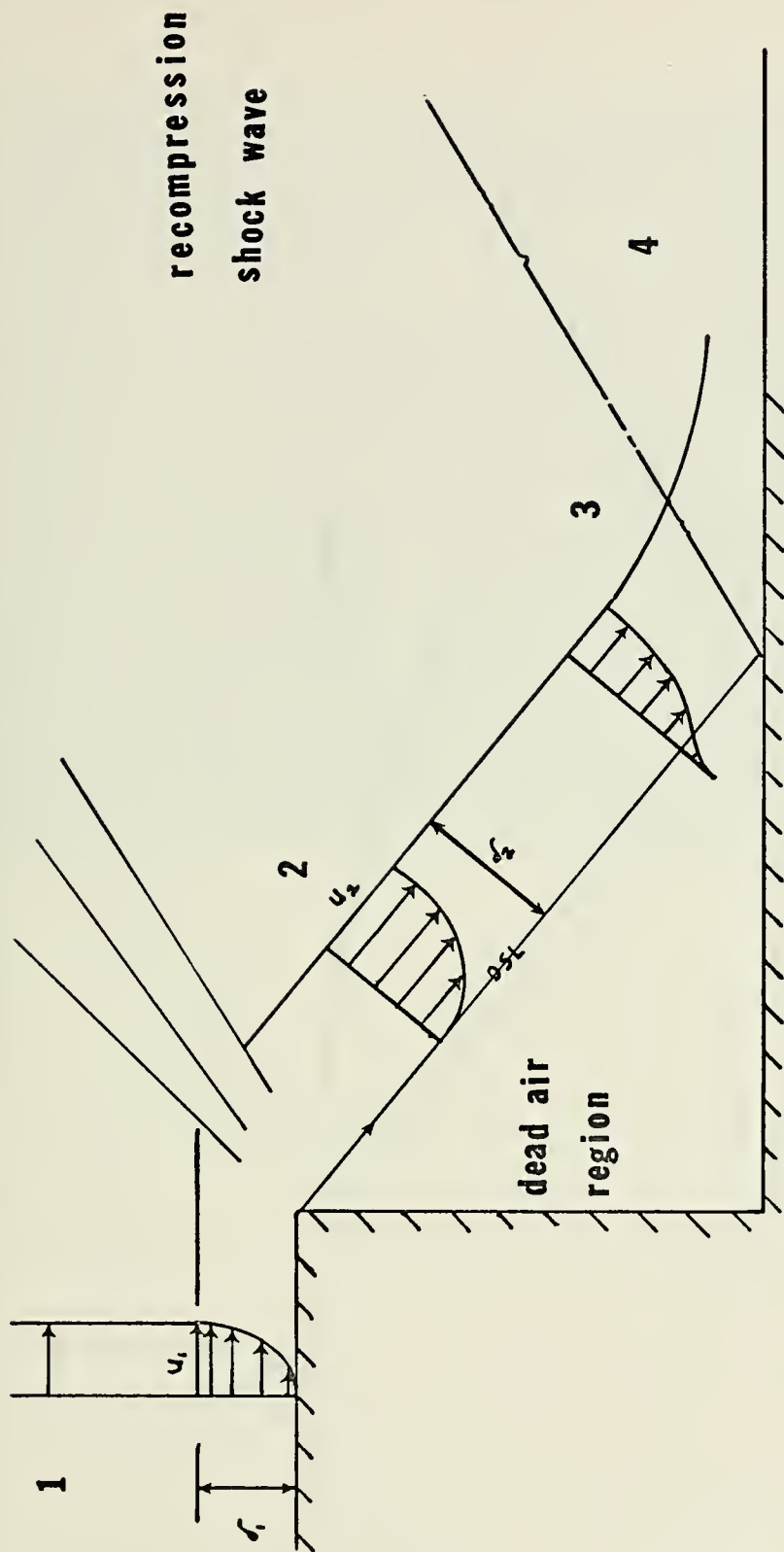


Figure 1. Chapman-Korst Flow Model for Supersonic Base Flow

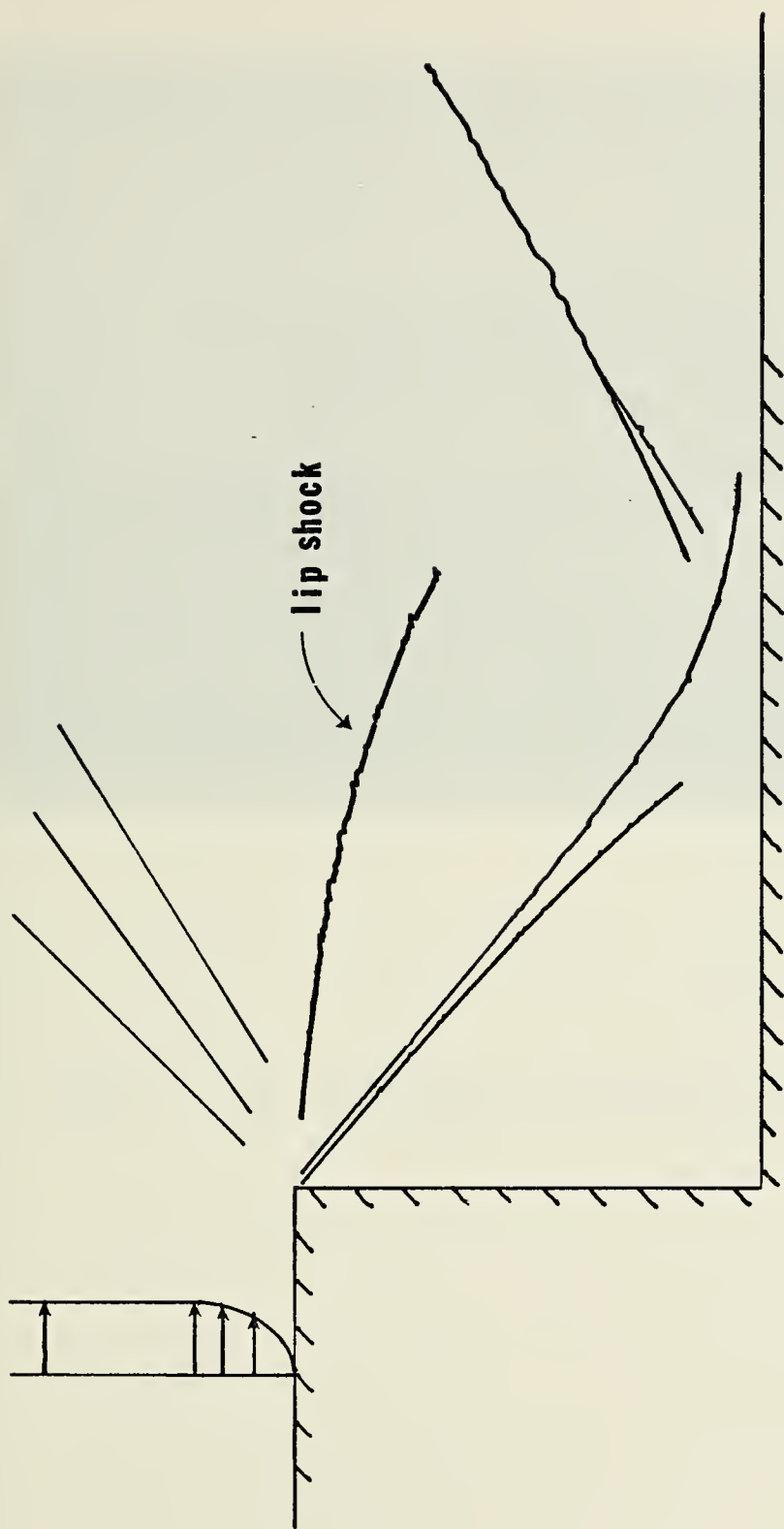


Figure 2. Lip Shock



Figure 3. The Experimental Model of a Rear-Facing Step.



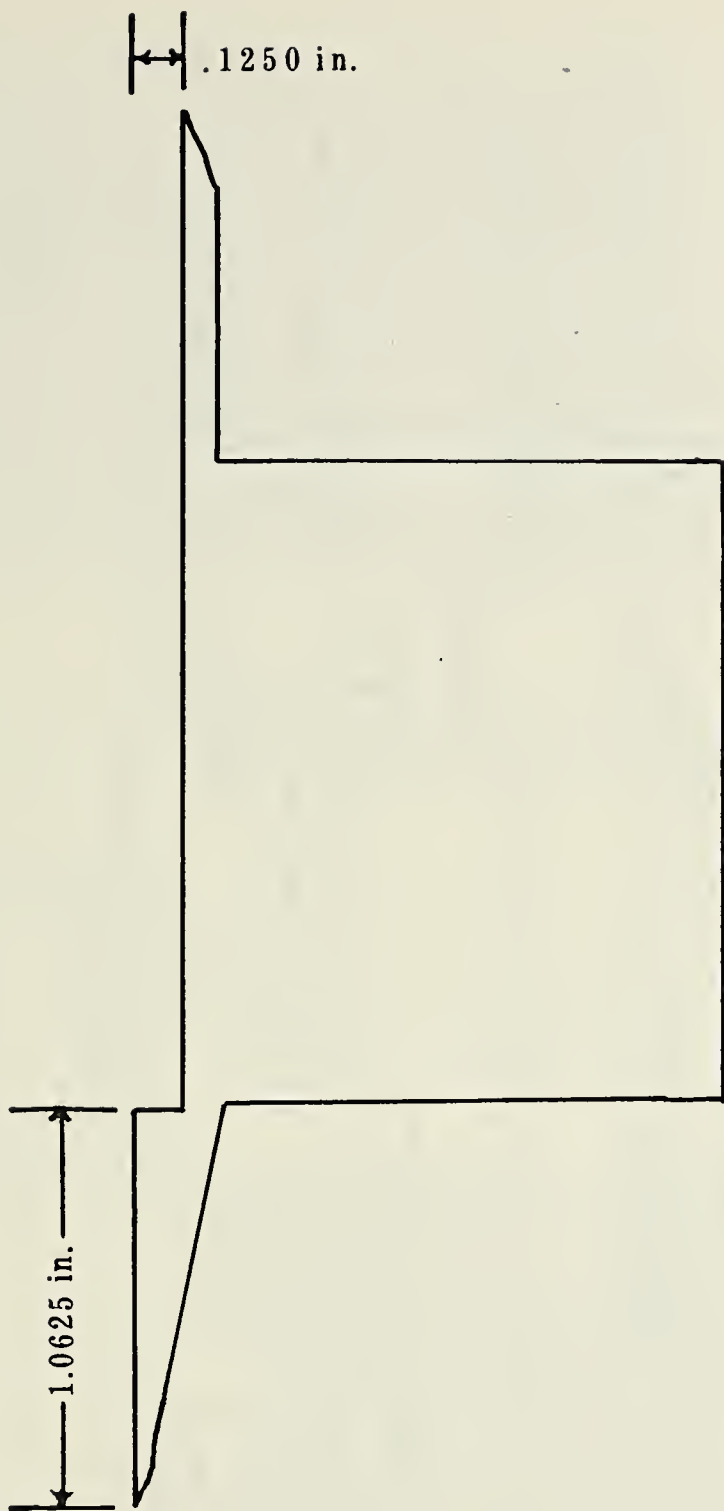


Figure 4. Experimental Model

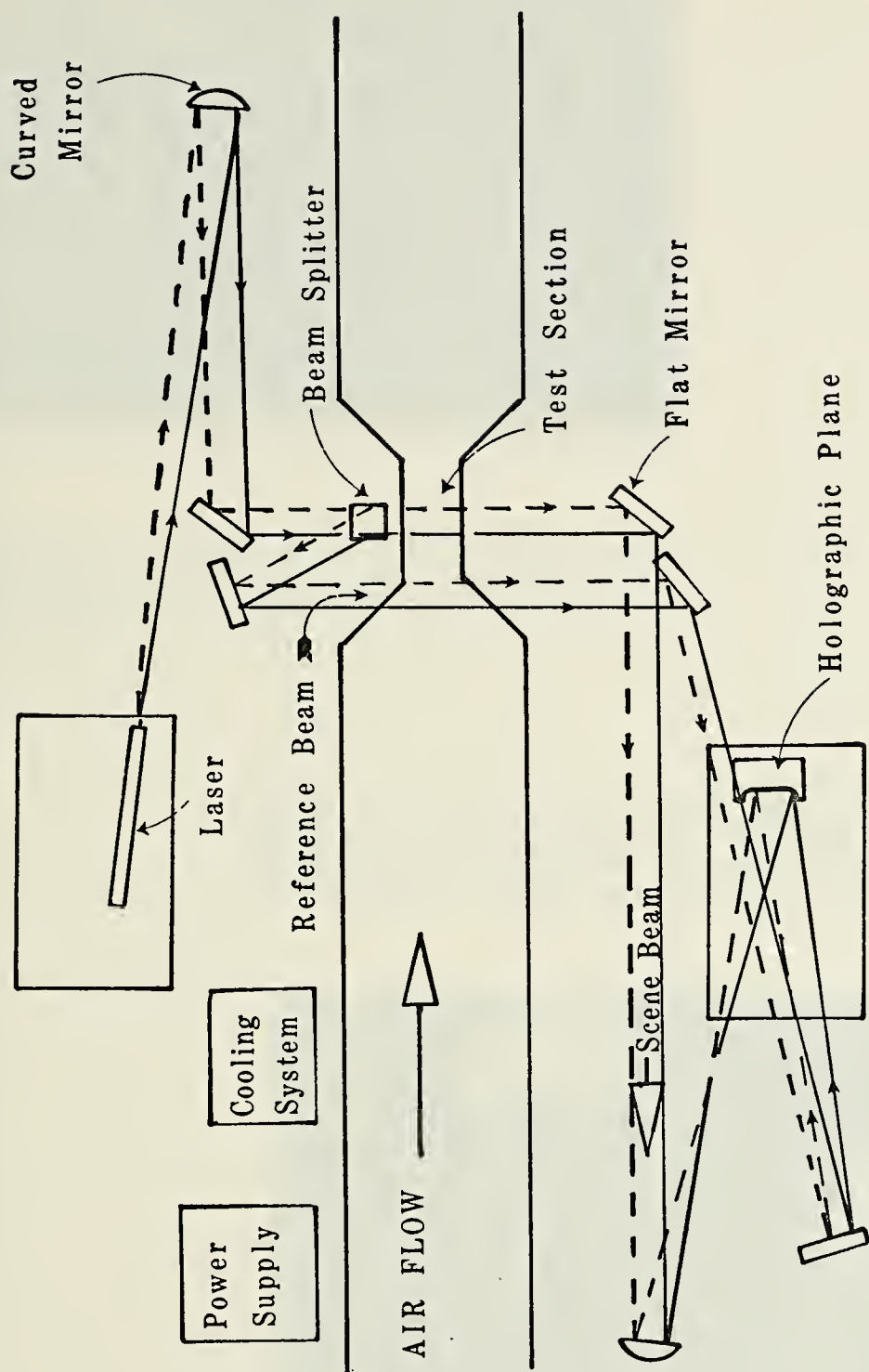


Figure 5. Experimental Setup

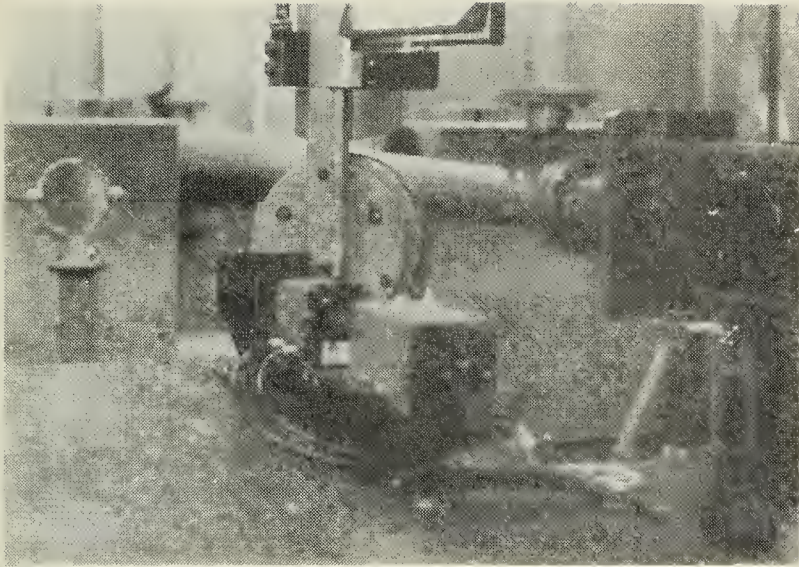
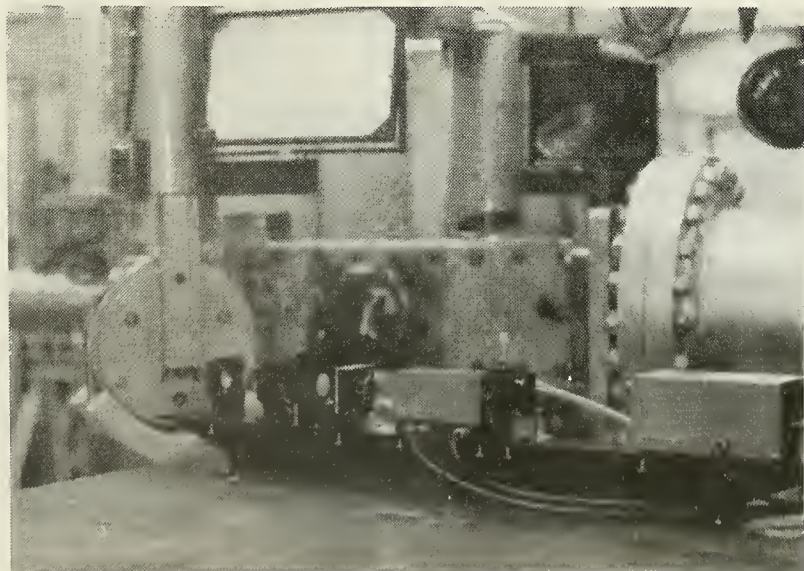


Figure 6. A view of the left side of the the experimental setup showing the laser and the optics system up to the beam splitter.

Figure 7. View of the left side of the test section, also showing the Q-switched laser, the beam splitter, and mirrors which direct the reference beam over the test section.



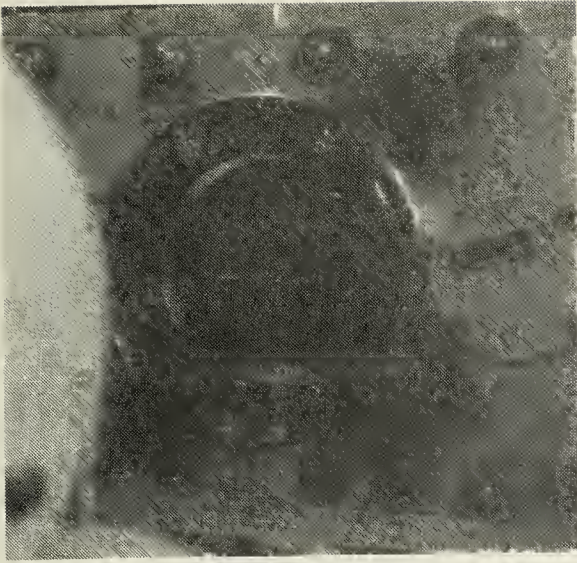
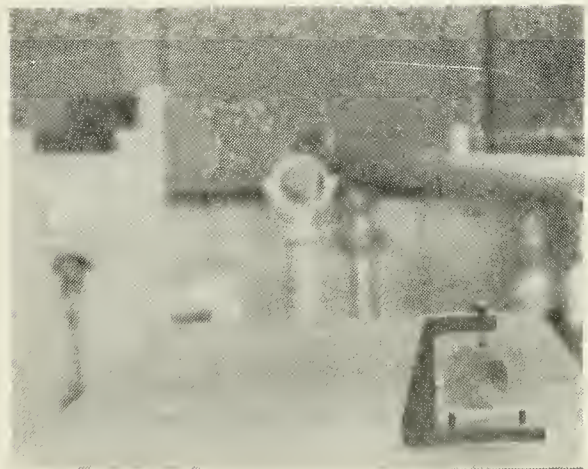


Figure 8.

A view of the right side
of the test section.

Figure 9.

A view of the right side
of the experimental setup
showing the holographic
plane and the final mirrors
for the reference and the
scene beams.



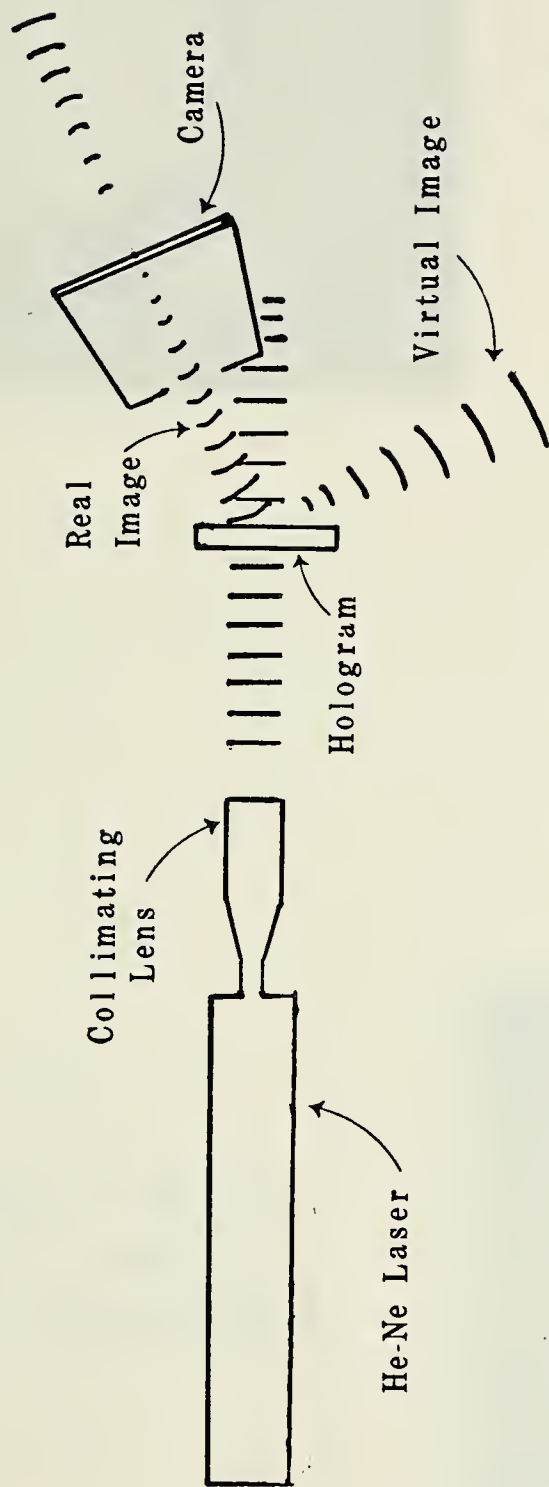


Figure 10. Reconstruction Setup

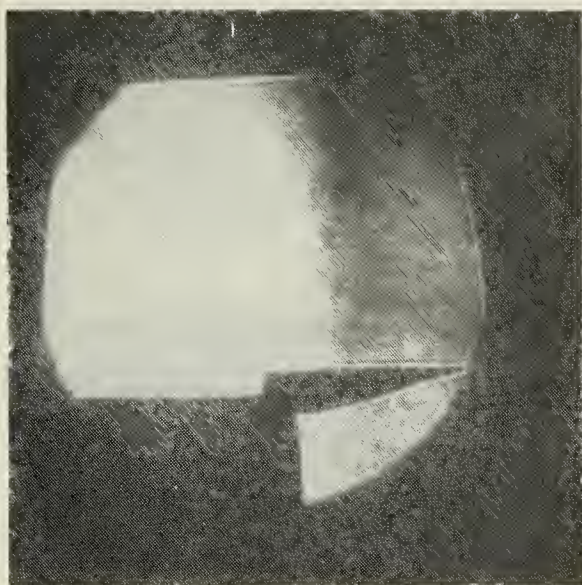


Figure 11.

Photograph of the projected real image of a single-exposed hologram.

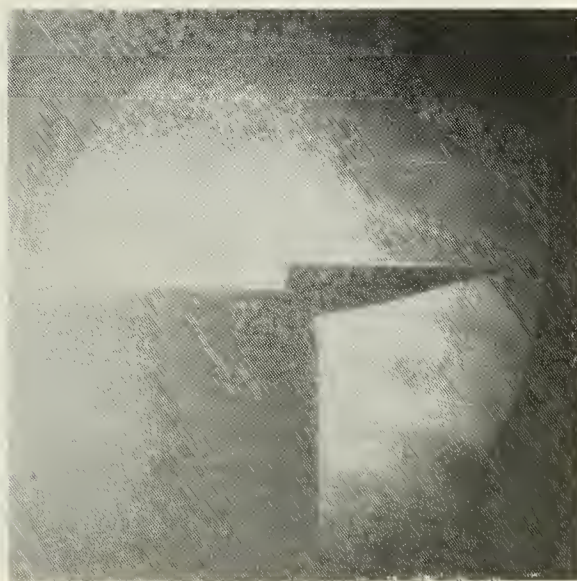


Figure 12.

Photograph of the projected real image of a single-exposed hologram.

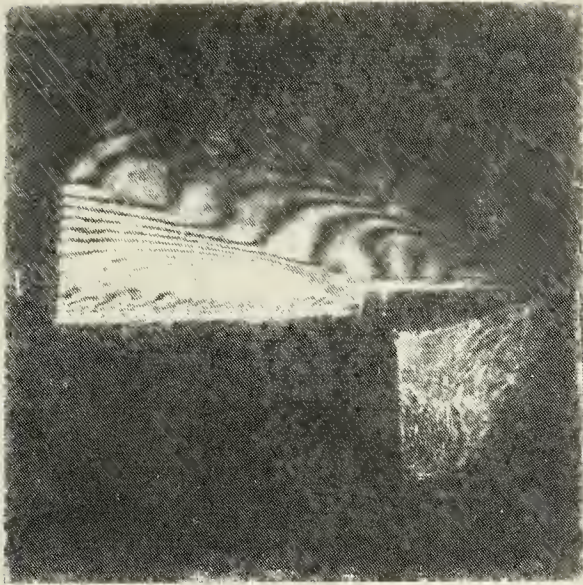
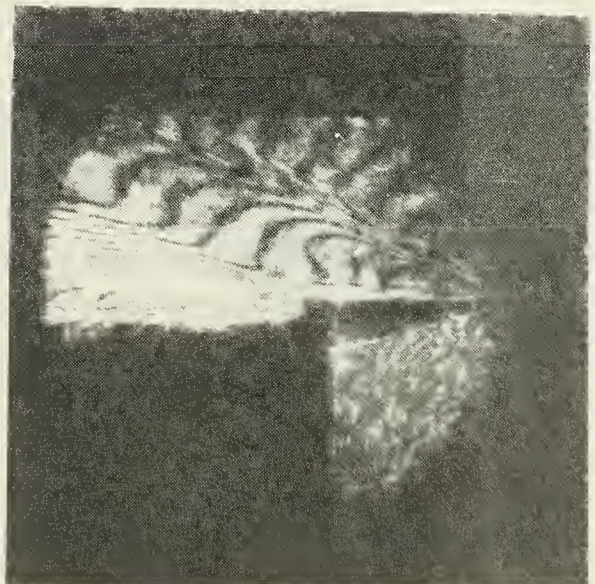


Figure 13.

Photograph of the projected real image of a double-exposed hologram of a rear-facing $1/8$ in. step in Mach 2.8 flow.

Figure 14.

Photograph of the projected real image of a double-exposed hologram of a rear-facing $1/8$ in. step in Mach 2.8 flow.



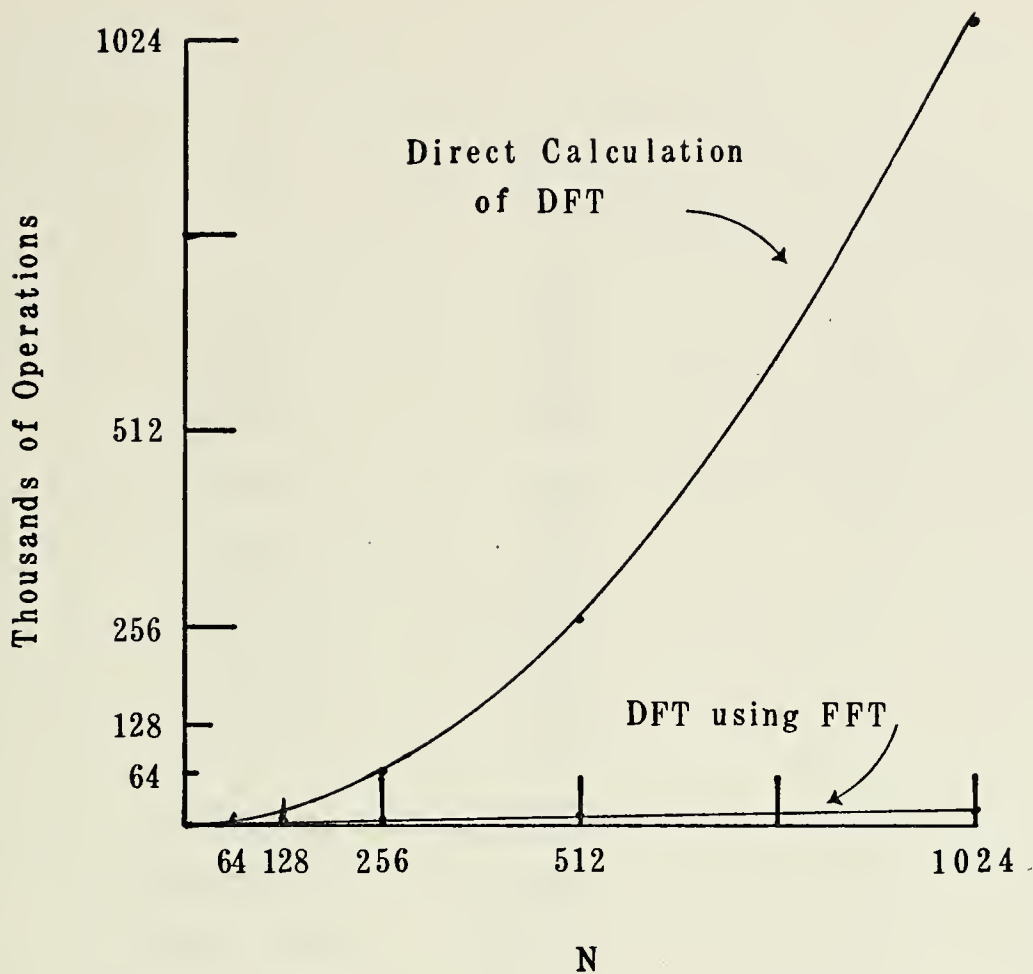


Figure 15. The Number of Operations Required to Compute the Discrete Fourier Transform by Direct Calculation Compared with Using the FFT Algorithm.

| Q | N | γ |
|-----------|-------|----------|
| 10 | 32 | 5 |
| 11-19 | 64 | 6 |
| 20-29 | 128 | 7 |
| 30-49 | 256 | 8 |
| 50-99 | 512 | 9 |
| 100-199 | 1024 | 10 |
| 200-299 | 2048 | 11 |
| 300-599 | 4096 | 12 |
| 600-999 | 8192 | 13 |
| 1000-1999 | 16384 | 14 |
| 2000-3999 | 32768 | 15 |

Optimum Value of N for FFT Convolution.

FIGURE 16.

APPENDIX A. DETAILED EXPERIMENTAL PROCEDURES

I. ALIGNMENT OF SYSTEM:

- a) Turn on cooling system and warm up power supply.
- b) Check internal alignment of laser with autocollimator.
- c) Insert 2.5 mm orifice inside laser cavity in order to eliminate higher order transverse mode emission.
- d) After ensuring all endangered personnel are wearing eye protectors, fire the Q-switch laser to burn a spot on underexposed (black) film.
- e) Make a needle hole in the center of the burn spot and fire the laser again to make a burn spot on another fixed piece of underexposed film. Always check for personnel wearing eye protectors prior to firing the Q-switch laser.
- f) Align a 15 mW CW laser beam through the 2.5 mm orifice and through the pin holes in the two pieces of film by using a flat mirror.
- g) Elevate table so that the laser beam hits the first mirror in the optics system in its center. Ensure that the focal point of the diffusing lens is located at the focal point of the parabolic mirror in order to obtain a collimated beam entering the optics system.
- h) Align optics system, ensuring test section and holographic plane are properly illuminated.
- i) Adjust the location of the holographic plane to ensure that the subject image is in focus in the diverging part of the scene beam.
- j) Adjust the final flat mirror in the reference beam in order to make sure path lengths of the two beams are within one-half inch of each other.

k) Remove CW laser and alignment mirror as well as remaining alignment pinholes.

1) Ready to fire.

II. EXPOSURE OF HOLOGRAPHIC PLATES:

a) Single Pulse (Exposure):

1) Insert plate in holder underneath the black drape.

2) Assistant charges the power supply and notifies experimenter when ready to fire.

3) Experimenter lifts the drape while simultaneously calling to fire the laser, and replaces the drape immediately after observing lamp flash of the Q-switch laser.

4) Remove the exposed holographic plate to a labeled film box while still under the drape to eliminate further exposure.

5) Hologram is ready for development.

b) Double-Pulse (Exposure):

1) Repeat steps II.a.1-3. Wear sound attenuators.

2) Open air supply and create desired flow in the test section.
(Mach 2.8 flow in this experiment)

3) Repeat steps II.a.2-5. Assistant shuts off air supply after firing laser.

APPENDIX B. INSIDE INTEGRAL SUBSECTION OF VAN HOUTEN'S COMPUTER PROGRAM

See Appendix E right hand count labeled EVE02460-2840 for location of this subsection in Van Houten's program.

```

*****CALCULATE VALUE OF INSIDE INTEGRAL *****
DC 43 I=1,NT
DC 43 J=1,NP
M=NPL+J
BD(1)=0.
DO 39 K=1,MAX
MKP=M+K
MKM=M-K
IF(MKP.GT.NPP) MKP=NPP
IF(MKM.LT.1) MKM=1
K1=K**2
39 BC(K+1)=(BB(MKP,I)+BB(MKM,I))-2.*BB(M,I)/(FLOAT(K1)*DR)
VAL=0.
K1=1
40 K2=K1+6
IF(K2.GT.MAX) GO TO 41
*****SIXTH ORDER QUADATURE FORMULA*****
VAL=VAL+C1*(BD(K1)+BD(K2))+C2*(BD(K1+1)+BD(K2-1))+C3*(BD(K1+2)+BD(K2-2))+C4*BD(K1+3)
K1=K2
GO TO 40
41 SUM=0.
*****CONTRIBUTION OF LAST TERM*****
DO 42 K=K1,MAX
SUM=SUM+BD(K)+BD(K+1)
42 SUM=COTES PLUS LAST TERMS PLUS INTEGRATION FROM 2 RMAX TO INFINITY
43 B(J,I)=VAL+SUM/2.-.666667*BB(M,I)/RMAX
IF(KSYM.LT.99) GO TO 48
*****03370
*****03390
*****03400
*****03410
*****03420
*****03430
*****03440
*****03450
*****03460
*****03470
*****03480
*****03490
*****03500
*****03510
*****03520
*****03530
*****03540
*****03550
*****03560
*****03570
*****03580
*****03590
*****03600
*****03610
*****03620
*****03630
*****03640
*****03650

```


APPENDIX C. FFT CONVOLUTION PROCEDURES

C.1 COMPUTATION PROCEDURE FOR FFT CONVOLUTION OF FINITE-LENGTH FUNCTIONS.

1. Let $x(t)$ and $h(t)$ be finite-length functions shifted from the origin by a and b , respectively.

2. Shift $x(t)$ and $h(t)$ to the origin and sample:

$$x(k) = x(KT + a) \quad k = 0, 1, \dots, P - 1$$

$$h(k) = h(KT + b) \quad k = 0, 1, \dots, Q - 1$$

3. Choose N to satisfy the relationships:

$$N \geq P + Q - 1$$

$$N = 2^{\text{integer valued}}$$

where P is the number of samples defining $x(t)$ and Q is the number of samples defining $h(t)$.

4. Augment with zeros the sampled functions of step (2).

$$x(k) = 0 \quad k = P, P + 1, \dots, N - 1$$

$$h(k) = 0 \quad k = Q, Q + 1, \dots, N - 1$$

5. Compute the discrete transform of $x(k)$ and $h(k)$.

$$X(n) = \sum_{k=0}^{N-1} x(k) \exp(-j2\pi nk/N)$$

$$H(n) = \sum_{k=0}^{N-1} h(k) \exp(-j2\pi nk/N)$$

6. Compute the product:

$$Y(n) = X(n)H(n)$$

7. Compute the inverse discrete transform using the forward transform:

$$y(k) = \sum_{n=0}^{N-1} \frac{1}{N} Y^*(n) \exp(-j2\pi nk/N)$$

C.2 COMPUTATION PROCEDURE FOR FFT CONVOLUTION: SELECT-SAVINGS METHOD:

1. Let Q be the number of samples representing $h(t)$.
2. Choose N according to the table in Figure 16.
3. Form the sampled periodic function $h(k)$.

$$\begin{aligned} h(k) &= h(kT) & k &= 0, 1, \dots, Q - 1 \\ &= 0 & k &= Q, Q + 1, \dots, N - 1 \end{aligned}$$

4. Compute the discrete Fourier transform of $h(k)$

$$H(n) = \sum_{k=0}^{N-1} h(k) \exp(-j2\pi nk/N)$$

5. Form the sampled periodic function:

$$x_1(k) = x(kT) \quad k = 0, 1, \dots, N - 1$$

6. Compute the discrete Fourier transform of $x_1(k)$.

$$X_1(n) = \sum_{k=0}^{N-1} x_1(k) \exp(-j2\pi nk/N)$$

7. Compute the product:

$$Y_1(n) = X_1(n)H(n)$$

8. Compute the inverse discrete transform of $Y_1(n)$.

$$y_1(k) = \sum_{n=0}^{N-1} \frac{1}{N} Y_1(n) \exp(-j2\pi nk/N)$$

9. Delete samples $y_1(0), y_1(1), \dots, y_1(Q - 2)$, and save the remaining samples.

10. Repeat steps 5 to 9 until all sections are computed.

11. Combine the sectioned results by the relationships:

$$\begin{aligned} y(k) &\text{ undefined} & k &= 0, 1, \dots, Q - 2 \\ y(k) &= y_1(k) & k &= Q - 1, Q, \dots, N - 1 \\ y(k+N) &= y_2(k+Q-1) & k &= 0, 1, \dots, N - Q \\ y(k+2N) &= y_3(k+Q-1) & k &= 0, 1, \dots, N - Q \end{aligned}$$

C.3 COMPUTATION PROCEDURE FOR FFT CONVOLUTION: OVERLAP-ADD METHOD.

1. Let Q be the number of samples representing $h(t)$.
2. Choose N according to the table in Figure 16.
3. Form the sampled periodic function $h(k)$:

$$\begin{aligned} h(k) &= h(kT) & k &= 0, 1, \dots, Q - 1 \\ &= 0 & k &= Q, Q + 1, \dots, N - 1 \end{aligned}$$

4. Compute the discrete Fourier transform of $h(k)$.

$$H(n) = \sum_{k=0}^{N-1} h(k) \exp(-j2\pi nk/N)$$

5. Form the sampled periodic function:

$$\begin{aligned} x_1(k) &= x(kT) & k &= 0, 1, \dots, N - Q \\ &= 0 & k &= N - Q + 1, \dots, N - 1 \end{aligned}$$

6. Compute the discrete Fourier transform of $x_1(k)$.

$$X_1(n) = \sum_{k=0}^{N-1} x_1(k) \exp(-j2\pi nk/N)$$

7. Compute the product:

$$Y_1(n) = X_1(n)H(n)$$

8. Compute the inverse discrete transform of $Y_1(n)$.

$$y_1(k) = \sum_{n=0}^{N-1} \frac{1}{N} Y_1(n) \exp(-j2\pi nk/N)$$

9. Repeat steps 5-8 until all sections are computed.
10. Combine the sectioned results by the relationships:

$$\begin{aligned} y(k) &= y_1(k) & k &= 0, 1, \dots, N - Q \\ y(k+N-Q+1) &= y_1(k+N-Q+1) + y_2(k) & k &= 0, 1, \dots, N - Q \\ y(k+2(N-Q+1)) &= y_2(k+N-Q+1) + y_3(k) & k &= 0, 1, \dots, N - Q \\ &\cdot \\ &\cdot \\ &\cdot \end{aligned}$$

APPENDIX D. SUBROUTINE CFFT2

```

.....
SUBROUTINE CFFT2      (CATEGORY E2)
PURPOSE
    TO COMPUTE THE COMPLEX FOURIER TRANSFORM OR INVERSE IN PLACE
    USING THE MIXED-RADIX FAST FOURIER TRANSFORM ALGORITHM. WITHIN
    CERTAIN LIMITATIONS, DISCUSSED BELOW, AN ARBITRARY NUMBER OF DATA
    POINTS MAY BE PROCESSED. SEE ROUTINE RFFT2 TO PROCESS REAL DATA
    IF THE NUMBER OF DATA POINTS IS EVEN.
USAGE
    CALL CFFT2 (A, B, NTOT, N, NSPAN, ISN)
DESCRIPTION OF PARAMETERS
    A - REAL*4 ARRAY HOLDING THE CONSECUTIVELY STORED REAL COM-
        PONENTS OF DATA (WHEN IABS(ISN) = 1) OR A COMPLEX*8
        ARRAY HOLDING DATA (WHEN IABS(ISN) = 2). AT EXIT FROM
        CFFT2, A WILL HOLD THE REAL COMPONENTS OF THE RESULTING
        REAL*4 FOURIER COEFFICIENTS WHEN IABS(ISN) = 1, OR THE
        COMPLEX*8 FOURIER COEFFICIENTS, WHEN IABS(ISN) = 2.
        SEE DESCRIPTION OF 'ISN' BELOW.
    B - WHEN IABS(ISN) = 1, B IS A REAL*4 ARRAY HOLDING THE CONSE-
        CUTIVELY STORED IMAGINARY COMPONENTS OF DATA. AT EXIT
        FROM CFFT2 IT WILL CONTAIN THE IMAGINARY COMPONENTS OF
        THE FOURIER COEFFICIENTS. WHEN USING COMPLEX*8 DATA
        (WHEN IABS(ISN) = 2) ALWAYS USE 'A(2)', INSTEAD OF 'B'. IN
        THE CALL STATEMENT, SINCE 'A' CONTAINS BOTH THE REAL AND
        IMAGINARY COMPONENTS OF DATA. SEE 'ISN' BELOW.
    NTOT - TOTAL NUMBER OF COMPLEX DATA VALUES INVOLVED. FCR A
        SINGLE-VARIABLE ANALYSIS, NTOT = N. NSPAN = (NUMBER
        OF COMPLEX DATA VALUES). FOR A TRI-VARIATE ANALYSIS
        OF 'A(N1,N2,N3)', AND 'B(N1,N2,N3)', WHERE IABS(ISN) = 1,
        OR COMPLEX 'A(N1,N2,N3)' WHERE IABS(ISN) = 2, NTOT
        WOULD BE THE PRODUCT, N1*N2*N3. (INTEGER*4)
        SEE "EXAMPLES" BELOW.

```

CC

CFFT0430
CFFT0440
CFFT0450
CFFT0460
CFFT0470
CFFT0480
CFFT0490
CFFT0500
CFFT0510
CFFT0520
CFFT0530
CFFT0540
CFFT0550
CFFT0560
CFFT0570
CFFT0580
CFFT0590
CFFT0600
CFFT0610
CFFT0620
CFFT0630
CFFT0640
CFFT0650
CFFT0660
CFFT0670
CFFT0680
CFFT0690
CFFT0700
CFFT0710
CFFT0720
CFFT0730
CFFT0740
CFFT0750
CFFT0760
CFFT0770
CFFT0780
CFFT0790
CFFT0800
CFFT0810
CFFT0820
CFFT0830
CFFT0840
CFFT0850
CFFT0860
CFFT0870
CFFT0880
CFFT0890
CFFT0900

N - DIMENSION OF CURRENT VARIABLE. IDENTICAL TO NTOT AND NSPAN AND THE NUMBER OF COMPLEX DATA VALUES IN SINGLE VARIABLE CASE. SEE "EXAMPLES" BELOW FOR CASES OF HIGHER DIMENSIONALITY. (INTEGER*4)

NSPAN - NSPAN/N IS THE SPACING OF CONSECUTIVE DATA VALUES WHEN INDEXING CURRENT VARIABLE. IT IS IDENTICAL TO NTOT AND N AND NC. CF COMPLEX DATA POINTS IN THE SINGLE-VARIABLE CASE. SEE "EXAMPLES" BELOW FOR MULTI-VARIABLE CASES. (INTEGER*4)

ISN - AN INTEGER*4 CONTROL VARIABLE BY WHICH USER SPECIFIES BOTH THE STORAGE MODE OF HIS DATA (AND RESULTING FOURIER COEFFICIENTS) AND WHETHER HE WANTS THE DISCRETE FOURIER TRANSFORM (DFT) OR THE INVERSE DISCRETE FOURIER TRANSFORM (IDFT).

IF ISN IS NEGATIVE THE DFT IS OBTAINED; IF ISN IS POSITIVE THE IDFT IS OBTAINED. IF ISN IS +1 OR -1, THE REAL COMPONENTS OF THE DATA SHOULD BE IN THE REAL*4 ARRAY 'A' AND THE IMAGINARY COMPONENTS IN THE REAL*4 ARRAY 'B'. BOTH OF WHICH SHOULD BE DIMENSIONED AT LEAST 'NTOT'. IF ISN IS +2 OR -2, THE COMPLEX DATA SHOULD BE STORED IN THE COMPLEX*8 ARRAY 'A' (AT LEAST NTOT IN LENGTH) AND THE SECOND ARGUMENT IN THE CALLING LIST SHOULD BE 'A(2)'.
H

REMARKS

DEFINITIONS: THE DISCRETE FOURIER TRANSFORM (DFT) OF $X(J)$ FOR $J=1(1)N$, IS $1/N$ TIMES THE SERIES GIVEN BY:

$$Y(K) = \sum_{J=1}^N X(J) * \exp(-2.*PI * I * J * K / N),$$

FOR $K = 1(1)N$.

(HERE "I" STANDS FOR $\sqrt{-1}$) AND $PI = 3.141593$.)

THE INVERSE DISCRETE FOURIER TRANSFORM (IDFT) OF $Y(J)$, $J=1,N$ IS THE SUMMATION FOR $K = 1(1)N$, OF THE TERMS,

$$Y(K) * \exp(2.*PI * I * J * K / N).$$

IMPORTANT NOTE: CFFT2 RETURNS THE UNNORMALIZED DFT WHEN ISN .LT. 0. THE RESULT VECTOR MUST BE DIVIDED BY N (NUMBER OF COMPLEX DATA POINTS) TO PRODUCE THE NORMALIZED DFT.

NOTES ON NUMBER OF DATA POINTS:

CC

THE MOST DISTINCTIVE FEATURE OF CFFT2 IS THAT IT ACCOMMODATES AN ALMOST ARBITRARY NUMBER OF DATA POINTS, EVEN THOUGH IT EMPLOYS THE COOLEY-TUKEY FAST FOURIER TRANSFORM ALGORITHM. HOWEVER CERTAIN LARGE PROBLEMS, MINOR ALTERATIONS TO THE SOURCE CODE MAY BE REQUIRED. AS IT STANDS CFFT2 WILL ACCOMMODATE ANY N. TO ANALYZE THE SITUATION FOR PRIME LARGER PROBLEMS THE USER SHOULD MAXIMIZE CFFT2 INTO ITS PRIME FACTORS. THE CONSTANT MAXF IN CFFT2 MUST BE CHANGED TO BE THE GREATEST PRIME FACTOR ON N (ONLY IF THIS IS BEING DONE). (GT. 997).

CFFT0910
CFFT0920
CFFT0930
CFFT0940
CFFT0950
CFFT0960
CFFT0970
CFFT0980
CFFT0990
CFFT1000

ALSO THE ARRAYS 'AT', 'CK', 'BT', AND 'SK' MUST BE
RE-DIMENSIONED TO BE AT LEAST MAXF IN LENGTH. N IS DEFINED AS SQUARED
THEN THE USER SHOULD COMPUTE K, WHICH OF N AFTER THE CONSTANT
THE PRODUCT OF THE REMAINING FACTORS IS. GT. 1, IF THE ARRAY NP
THE FACTORS ARE STRUCK OUT. IF K IS AT LEAST K-1, AND THE NUMBER OF
MAXP MUST BE ALTERED TO BE AT LEAST K-1, AND THE NUMBER OF
MUST BE RE-DIMENSIONED TO MAXP. N IS GT. 15, THE ARRAY NFAC
FACTORS (TO THE FIRST POWER) IF AVAILABLE STORAGE IS
FACTORS BE INCREASED THAT NUMBER. IF A STORAGE STATEMENT.
INSUFFICIENT, CFFT2 TERMINATES VIA A STOP 99 STATEMENT.

NOTE: FOR LARGE PROBLEMS REQUIRING ALTERATIONS DESCRIBED ABOVE, THE USER MAY HAVE TO SUBSTITUTE THE DCUBLE-PRECISION VERSION OF CFFT2, (DCFFT2). SEE EXAMPLE BELOW FOR ACCURACY TEST.

EXAMPLES

```

      TO OBTAIN DFT OF SINGLE-VARIABLE DATA STORED IN A
      COMPLEX#8 ARRAY, A:
      CALL CFFT2 (A, A(2), N, N, N, -2)

```

TO OBTAIN THE DFT OF TRI-VARIATE DATA AT A(N1,N2,N3) (REAL COMPONENTS) AND B(N1,N2,N3) (IMAGINARY COMPONENTS):

NOTE: THREE CALLS OF CFFT2 ARE REQUIRED.


```

CCCCCCCCCCCCCCCCCCCCCCCCCCCCCCCCCCCCCCCCCCCCCCCCCCCCCCCCCCCC
CALL CFFT2 (A, A(2), N, N, N, -2)
CALL CFFT2 (A, A(2), N, N, N, 2)
FN= N
DO 33 I = 1, N
  33 A(I) = A(I)/ FN
N.B. FINAL DATA IN 'A' WOULD BE IDENTICAL TO ORIGINAL DATA,
IF NO ACCURACY WERE LCST. AN EXPERIMENTAL CALCULATION
OF THIS SCRT MAY REVEAL THE NECESSITY OF PERFECTING
YOUR CALCULATIONS IN DCUBLE PRECISION. (SEE DCFFT2.)
SIZE: 53K BYTES, INCLUDING SYSTEM ROUTINES AND EXCLUDING DATA.
SUBROUTINES/FUNCTIONS REQUIRED
ONLY BUILT-IN FORTRAN FUNCTIONS ARE REQUIRED.
METHOD/REFERENCES
1.) SINGLETON, R.C., "AN ALGRITM FOR CCPUTING THE MIXED
RADIO FAST FOURIER TRANSFORM," IEEE TRANSACTIONS ON
AUDIO AND ELECTROACOUSTICS, 17(2), JUNE 1969, PP. 93-103.
2.) RITEA, H.B., "A COMPARISON OF FFT ALGORITHMS," SYS DEV
CORP, 5 JAN 1972, PP. 9-20. (AD 735-920) (TM4857/100).
PROGRAMMER: R. C. SINGLETON, S.R.I., OCT. 1968
IMPLEMENTER AT NPS: R. R. HILLEARY, MARCH 1973
SUBROUTINE CFFT2(A,B,NTOT,N,NSPAN,ISN)
DIMENSION A(N), B(N)
DIMENSION NFAC(15), NP(1000)
DIMENSION AT(1000), CK(1000), BT(1000), SK(1000)
EQUIVALENCE (I,II)
THE FOLLOWING CONSTANT SHOULD MATCH ARRAYS' DIMENSION
MAXF = 997
THE FOLLOWING CONSTANT MAY ALSO NEED ADJUSTMENT. SEE WRITEUP.
MAXP = 1000
IF (N .LT. 2) RETURN
INC = ISN
RAD = 6.28318531D0
S72 = RAD/5.
C72 = COS(S72)
CFFT1390
CFFT1400
CFFT1410
CFFT1420
CFFT1430
CFFT1440
CFFT1450
CFFT1460
CFFT1470
CFFT1480
CFFT1490
CFFT1500
CFFT1510
CFFT1520
CFFT1530
CFFT1540
CFFT1550
CFFT1560
CFFT1570
CFFT1580
CFFT1590
CFFT1600
CFFT1610
CFFT1620
CFFT1630
CFFT1640
CFFT1650
CFFT1660
CFFT1670
CFFT1680
CFFT1690
CFFT1700
CFFT1710
CFFT1720
CFFT1730
CFFT1740
CFFT1750
CFFT1760
CFFT1770
CFFT1780
CFFT1790
CFFT1800
CFFT1810
CFFT1820
CFFT1830
CFFT1840
CFFT1850
CFFT1860

```



```

C      S72 = SIN(S72)
      S120 = .8660254D0
      IF (ISN .GE. 0) GO TO 10
      S72 = -S72
      S120 = -S120
      RAD = -RAD
      INC = -INC
C
C      10 NT = INC * NTOT
      KS = INC * NSPAN
      KSPAN = KS
      NN = NT - INC
      JC = KS/NN
      RADF = RAD * FLOAT(JC) * .5
      I = 0
      JF = 0
C
C      DETERMINE FACTORS OF N
C
C      M = 0
      K = N
      GC TO 20
C
C      15 M = M + 1
      NFAC(M) = 4
      K = K/16
C
C      20 IF (K - (K/16) * 16 .EQ. 0) GO TO 15
      J = 3
      JJ = 9
      GC TO 30
C
C      25 M = M + 1
      NFAC(M) = J
      K = K/JJ
C
C      30 IF (MOD(K,JJ) .EQ. 0) GO TO 25
      J = J + 2
      JJ = J**2
      IF (JJ .LE. K) GO TO 30
      IF (K .GT. 4) GO TO 40
      KT = M
      NFAC(M+1) = K
      IF (K .NE. 1) M = M+1
      GC TO 80
C
C      40 IF (K - (K/4)*4 .NE. 0) GO TO 50

```

```

CFFFT1870
CFFFT1880
CFFFT1890
CFFFT1900
CFFFT1910
CFFFT1920
CFFFT1930
CFFFT1940
CFFFT1950
CFFFT1960
CFFFT1970
CFFFT1980
CFFFT1990
CFFFT2000
CFFFT2010
CFFFT2020
CFFFT2030
CFFFT2040
CFFFT2050
CFFFT2060
CFFFT2070
CFFFT2080
CFFFT2090
CFFFT2100
CFFFT2110
CFFFT2120
CFFFT2130
CFFFT2140
CFFFT2150
CFFFT2160
CFFFT2170
CFFFT2180
CFFFT2190
CFFFT2200
CFFFT2210
CFFFT2220
CFFFT2230
CFFFT2240
CFFFT2250
CFFFT2260
CFFFT2270
CFFFT2280
CFFFT2290
CFFFT2300
CFFFT2310
CFFFT2320
CFFFT2330
CFFFT2340

```


CFFT2350
 CFFT2360
 CFFT2370
 CFFT2380
 CFFT2390
 CFFT2400
 CFFT2410
 CFFT2420
 CFFT2430
 CFFT2440
 CFFT2450
 CFFT2460
 CFFT2470
 CFFT2480
 CFFT2490
 CFFT2500
 CFFT2510
 CFFT2520
 CFFT2530
 CFFT2540
 CFFT2550
 CFFT2560
 CFFT2570
 CFFT2580
 CFFT2590
 CFFT2600
 CFFT2610
 CFFT2620
 CFFT2630
 CFFT2640
 CFFT2650
 CFFT2660
 CFFT2670
 CFFT2680
 CFFT2690
 CFFT2700
 CFFT2710
 CFFT2720
 CFFT2730
 CFFT2740
 CFFT2750
 CFFT2760
 CFFT2770
 CFFT2780
 CFFT2790
 CFFT2800
 CFFT2810
 CFFT2820

```

      M = M + 1
      NFAC(M) = 2
      K = K/4
    50 KT = M
      J = 2
    60 IF (MOD(K,J) .NE. 0) GO TO 70
      M = M+1
      NFAC(M) = J
      K = K/J
    70 J = ((J+1)/2)*2 + 1
      IF (J .LE. K) GO TO 60
    80 IF (KT .EQ. 0) GO TO 100
      J = KT
    90 M = M+1
      NFAC(M) = NFAC(J)
      J = J-1
      IF (J .NE. 0) GO TO 90
      COMPUTE FOURIER TRANSFORM
    100 SD = RADF/ FLGAT(KSPAN)
      CC = 2.0 * SIN(SD)**2
      SD = SIN(SD+SD)
      KK = 1
      I = I + 1
      IF (NFAC(I) .NE. 2) GO TO 400
      TRANSFORM FOR FACTOR OF 2 (INCLUDING RTATION FACTOR)
      KSPAN = KSPAN/2
      K1 = KSPAN + 2
    210 K2 = KK + KSPAN
      AK = A(K2)
      BK = B(K2)
      A(K2) = A(KK) - AK
      B(K2) = B(KK) - BK
      A(KK) = A(KK) + AK
      B(KK) = B(KK) + BK
      KK = K2 + KSPAN
      IF (KK .LE. NN) GO TO 210
      KK = KK - NN
  
```



```

C 220 C1 = 1.0 -CD
      S1 = SD
      IF (KK .LE. JC) GO TO 210
      IF (KK .GT. KSPAN) GO TO 800

C 230 K2 = KK + KSPAN
      AK = A(KK) - A(K2)
      BK = B(KK) - B(K2)
      A(KK) = A(KK) + A(K2)
      B(KK) = B(KK) + B(K2)
      A(K2) = C1 * AK - S1 * BK
      B(K2) = S1 * AK + C1 * BK
      KK = K2 + KSPAN
      IF (KK .LT. NT) GO TO 230
      K2 = KK - NT
      C1 = -C1
      KK = K1 - K2
      IF (KK .GT. K2) GO TO 230
      AK = C1 - (CD * C1 - CD * S1) + S1
      S1 = (SD * C1 - CD * S1) + S1

C C1 = 0.5 / (AK**2 + S1**2) + 0.5
      S1 = C1 * S1
      C1 = C1 * AK
      KK = KK + JC
      IF (KK .LT. K2) GO TO 230

C K1 = K1 + INC + INC
      KK = (K1 - KSPAN) / 2 + JC
      IF (KK .LE. JC+JC) GO TO 220
      GC TO 100

C TRANSFORM FOR FACTOR OF 3

C 320 K1 = KK + KSPAN
      K2 = K1 + KSPAN
      AK = A(KK)
      BK = B(KK)
      AJ = A(K1) + A(K2)
      BJ = B(K1) + B(K2)
      A(KK) = AK + AJ
      B(KK) = BK + BJ
      AK = -0.5 * AJ + AK
      BK = -0.5 * BJ + BK
      AJ = (A(K1) - A(K2)) * S120
      BJ = (B(K1) - B(K2)) * S120

```

```

CFFFT2830
CFFFT2840
CFFFT2850
CFFFT2860
CFFFT2870
CFFFT2880
CFFFT2890
CFFFT2900
CFFFT2910
CFFFT2920
CFFFT2930
CFFFT2940
CFFFT2950
CFFFT2960
CFFFT2970
CFFFT2980
CFFFT2990
CFFFT3000
CFFFT3010
CFFFT3020
CFFFT3030
CFFFT3040
CFFFT3050
CFFFT3060
CFFFT3070
CFFFT3080
CFFFT3090
CFFFT3100
CFFFT3110
CFFFT3120
CFFFT3130
CFFFT3140
CFFFT3150
CFFFT3160
CFFFT3170
CFFFT3180
CFFFT3190
CFFFT3200
CFFFT3210
CFFFT3220
CFFFT3230
CFFFT3240
CFFFT3250
CFFFT3260
CFFFT3270
CFFFT3280
CFFFT3290
CFFFT3300

```



```

C      A(K1) = AK - BJ
C      B(K1) = BK + AJ
C      A(K2) = AK + BJ
C      B(K2) = BK - AJ
C      KK = K2 + KSPAN
C      IF (KK.LT.NN) GO TO 320
C      IF (KK.LE.NN) KSPAN) GO TO 320
C      GO TO 700
C
C      TRANSFORM FOR FACTOR OF 4
C
C      400 IF (NFAC(I).NE.4) GO TO 600
C      KSPNN = KSPAN
C      KSPAN = KSPAN/4
C
C      410 C1 = 1.0
C      S1 = 0.0
C
C      420 K1 = KK + KSPAN
C      K2 = K1 + KSPAN
C      K3 = K2 + KSPAN
C      AKP = A(KK) + A(K2)
C      AKM = A(KK) - A(K2)
C      AJP = A(K1) + A(K3)
C      AJM = A(K1) - A(K3)
C      A(KK) = AKP + AJP
C      AJP = AKP - AJP
C
C      BKP = B(KK) + B(K2)
C      BKM = B(KK) - B(K2)
C      BJP = B(K1) + B(K3)
C      BJM = B(K1) - B(K3)
C      B(KK) = BKP + BJP
C      BJP = BKP - BJP
C
C      IF (ISN.LT.0) GO TO 450
C      AKP = AKM - BJM
C      AKM = AKM + BJM
C
C      BKP = BKM + AJM
C      BKM = BKM - AJM
C      IF (S1.EQ.0.0) GO TO 460
C
C      430 A(K1) = AKP*C1 - BKP*S1
C      B(K1) = AKP*S1 + BKP*C1
C
C      A(K2) = AJP*C2 - BJP*S2

```

```

CFFT33310
CFFT33320
CFFT33330
CFFT33340
CFFT33350
CFFT33360
CFFT33370
CFFT33380
CFFT33390
CFFT33400
CFFT33410
CFFT33420
CFFT33430
CFFT33440
CFFT33450
CFFT33460
CFFT33470
CFFT33480
CFFT33490
CFFT33500
CFFT33510
CFFT33520
CFFT33530
CFFT33540
CFFT33550
CFFT33560
CFFT33570
CFFT33580
CFFT33590
CFFT33600
CFFT33610
CFFT33620
CFFT33630
CFFT33640
CFFT33650
CFFT33660
CFFT33670
CFFT33680
CFFT33690
CFFT33700
CFFT33710
CFFT33720
CFFT33730
CFFT33740
CFFT33750
CFFT33760
CFFT33770
CFFT33780

```



```

C      B(K2) = AJP*S2 + BJP*C2
C      A(K3) = AKM*C3 - BKM*S3
C      B(K3) = AKM*S3 + BKM*C3
C      KK = K3 + KSPAN
C      IF (KK.LE. NT) GO TO 420
C      440 G2 = C1 - (CD*C1 + SD*S1)
C      S1 = (SD*C1 - CD*S1) + S1
C      C1 = 0.5/(C2**2 + S1**2) + 0.5
C      S1 = C1*S1
C      C2 = C1**2 - S1**2
C      S2 = 2.0*C1*S1
C      C3 = C2**2 - S2**2
C      S3 = C2*S1 + S2*S1
C      KK = KK - NT + JC
C      IF (KK.LE. KSPAN) GO TO 420
C      KK = KK - KSPAN + INC
C      IF (KK.LE. JC) GO TO 410
C      IF (KSPAN.EQ. JC) GO TO 800
C      GO TO 100
C      450 AKP = AKM + BJM
C      AKM = AKM - BJM
C      BKP = BKM - AJM
C      BKM = BKM + AJM
C      IF (S1.NE. 0.0) GO TO 430
C      460 A(K1) = AKP
C      B(K1) = BKP
C      A(K2) = AJP
C      B(K2) = BJP
C      A(K3) = AKM
C      B(K3) = BKM
C      KK = K3 + KSPAN
C      IF (KK.LE. NT) GO TO 420
C      GO TO 440

```

TRANSFORM FOR A FACTOR OF 5.

```

CFFT3790
CFFT3800
CFFT3810
CFFT3820
CFFT3830
CFFT3840
CFFT3850
CFFT3860
CFFT3870
CFFT3880
CFFT3890
CFFT3900
CFFT3910
CFFT3920
CFFT3930
CFFT3940
CFFT3950
CFFT3960
CFFT3970
CFFT3980
CFFT3990
CFFT4000
CFFT4010
CFFT4020
CFFT4030
CFFT4040
CFFT4050
CFFT4060
CFFT4070
CFFT4080
CFFT4090
CFFT4100
CFFT4110
CFFT4120
CFFT4130
CFFT4140
CFFT4150
CFFT4160
CFFT4170
CFFT4180
CFFT4190
CFFT4200
CFFT4210
CFFT4220
CFFT4230
CFFT4240
CFFT4250
CFFT4260

```


510 C2 = C72**2 - S72**2
S2 = 2.0 * C72 * S72

C

520 K1 = KK + KSPAN
K2 = K1 + KSPAN
K3 = K2 + KSPAN
K4 = K3 + KSPAN

C

AKP = A(K1) + A(K4)
AKM = A(K1) - A(K4)
BKM = B(K1) + B(K4)
BKM = B(K1) - B(K4)

C

AJP = A(K2) + A(K3)
AJM = A(K2) - A(K3)
EJM = B(K2) + B(K3)
BJM = B(K2) - B(K3)

C

AA = A(KK)
BE = B(KK)
A(KK) = AA + AKP + AJP
B(KK) = BB + BKP + BJP

C

AK = AKP * C72 + AJP * C2 + AA
BK = BKP * C72 + BJP * C2 + BB
AJ = AKM * S72 + AJM * S2
BJ = BKM * S72 + BJM * S2

C

A(K1) = AK - BJ
A(K4) = AK + BJ
B(K1) = BK + AJ
B(K4) = BK - AJ

C

AK = AKP * C2 + AJP * C72 + AA
BK = BKP * C2 + BJP * C72 + BB
AJ = AKM * S2 - AJM * S72
BJ = BKM * S2 - BJM * S72

C

A(K2) = AK - BJ
A(K3) = AK + BJ
B(K2) = BK + AJ
B(K3) = BK - AJ
KK = K4 + KSPAN

C

IF (KK .LT. NN) GO TO 520
KK = KK - NN

C

IF (KK .LE. KSPAN) GO TO 520

CFFT4270
CFFT4280
CFFT4290
CFFT4300
CFFT4310
CFFT4320
CFFT4330
CFFT4340
CFFT4350
CFFT4360
CFFT4370
CFFT4380
CFFT4390
CFFT4400
CFFT4410
CFFT4420
CFFT4430
CFFT4440
CFFT4450
CFFT4460
CFFT4470
CFFT4480
CFFT4490
CFFT4500
CFFT4510
CFFT4520
CFFT4530
CFFT4540
CFFT4550
CFFT4560
CFFT4570
CFFT4580
CFFT4590
CFFT4600
CFFT4610
CFFT4620
CFFT4630
CFFT4640
CFFT4650
CFFT4660
CFFT4670
CFFT4680
CFFT4690
CFFT4700
CFFT4710
CFFT4720
CFFT4730
CFFT4740


```

C
C      GO TO 700
C      TRANSFORM FOR ODD FACTORS.
C
C      600 K = NFAC(I)
C          KSPNN = KSPAN
C          KSPAN = KSPAN/K
C          IF (K .EQ. 3) GO TO 320
C
C          IF (K .EQ. 5) GO TO 510
C
C          IF (K .EQ. JF) GO TO 640
C
C          JF = K
C          S1 = RAD/FLOAT(K)
C          C1 = COS(S1)
C          S1 = SIN(S1)
C          IF (JF .GT. MAXF) GO TO 998
C
C          CK(JF) = 1.0
C          SK(JF) = 0.0
C          J = 1
C
C      630 CK(J) = CK(K) * C1 + SK(K) * S1
C          SK(J) = CK(K) * S1 - SK(K) * C1
C
C          K = K - 1
C          CK(K) = CK(J)
C          SK(K) = -SK(J)
C
C          J = J + 1
C          IF (J .LT. K) GO TO 630
C
C      640 K1 = KK
C          K2 = KK + KSPNN
C
C          AA = A(KK)
C          BB = B(KK)
C          AK = AA
C          BK = BB
C
C          J = 1
C          K1 = K1 + KSPAN
C
C      650 K2 = K2 - KSPAN
C          J = J + 1
C          AT(J) = A(K1) + A(K2)

```

```

CFFT4750
CFFT4760
CFFT4770
CFFT4780
CFFT4790
CFFT4800
CFFT4810
CFFT4820
CFFT4830
CFFT4840
CFFT4850
CFFT4860
CFFT4870
CFFT4880
CFFT4890
CFFT4900
CFFT4910
CFFT4920
CFFT4930
CFFT4940
CFFT4950
CFFT4960
CFFT4970
CFFT4980
CFFT4990
CFFT5000
CFFT5010
CFFT5020
CFFT5030
CFFT5040
CFFT5050
CFFT5060
CFFT5070
CFFT5080
CFFT5090
CFFT5100
CFFT5110
CFFT5120
CFFT5130
CFFT5140
CFFT5150
CFFT5160
CFFT5170
CFFT5180
CFFT5190
CFFT5200
CFFT5210
CFFT5220

```



```

CFFFT5230
CFFFT5240
CFFFT5250
CFFFT5260
CFFFT5270
CFFFT5280
CFFFT5290
CFFFT5300
CFFFT5310
CFFFT5320
CFFFT5330
CFFFT5340
CFFFT5350
CFFFT5360
CFFFT5370
CFFFT5380
CFFFT5390
CFFFT5400
CFFFT5410
CFFFT5420
CFFFT5430
CFFFT5440
CFFFT5450
CFFFT5460
CFFFT5470
CFFFT5480
CFFFT5490
CFFFT5500
CFFFT5510
CFFFT5520
CFFFT5530
CFFFT5540
CFFFT5550
CFFFT5560
CFFFT5570
CFFFT5580
CFFFT5590
CFFFT5600
CFFFT5610
CFFFT5620
CFFFT5630
CFFFT5640
CFFFT5650
CFFFT5660
CFFFT5670
CFFFT5680
CFFFT5690
CFFFT5700

```

```

C      AK = AT(J) + AK
      BT(J) = B(K1) + B(K2)
      BK = BT(J) + BK
      J = J+1
C
C      AT(J) = A(K1) - A(K2)
      BT(J) = B(K1) - B(K2)
C
C      K1 = K1 + KSPAN
      IF (K1.LT.K2) GO TO 650
C
C      A(KK) = AK
      B(KK) = BK
C
C      K1 = KK
      K2 = KK + KSPNN
      J = 1
C
C      66C  K1 = K1 + KSPAN
           K2 = K2 - KSPAN
           JJ = J
C
C      AK = AA
      BK = BB
      AJ = 0.0
      BJ = 0.0
      K = 1
C
C      670  K = K + 1
           AK = AT(K) * CK(JJ) + AK
           BK = BT(K) * CK(JJ) + BK
C
C      K = K + 1
      AJ = AT(K) * SK(JJ) + AJ
      BJ = BT(K) * SK(JJ) + BJ
C
C      JJ = JJ + J
      IF (JJ.GT.JF) JJ = JJ - JF
C
C      IF (K.LT.JF) GO TO 670
C
C      K = JF - J
      A(K1) = AK - BJ
      B(K1) = BK + AJ
C
C      A(K2) = AK + BJ
      B(K2) = BK - AJ

```



```

C      J = J + 1
C      IF (J .LT. K) GO TO 660
C      KK = KK + KSPNN
C      IF (KK .LE. NN) GO TO 640
C      KK = KK - NN
C      IF (KK .LE. KSPAN) GO TO 640
C      MULTIPLY BY ROTATION FACTOR (EXCEPT FOR FACTORS OF 2 AND 4).
C      700 IF (I .EQ. M) GO TO 800
C      KK = JC + 1
C      710 C2 = 1.0 - CD
C      S1 = SD
C      720 C1 = C2
C      S2 = S1
C      KK = KK + KSPAN
C      730 AK = A(KK)
C      A(KK) = C2 * AK - S2 * B(KK)
C      B(KK) = S2 * AK + C2 * B(KK)
C      KK = KK + KSPNN
C      IF (KK .LE. NT) GO TO 730
C      AK = S1 * S2 + C1 * S2
C      S2 = S1 * C2 - AK
C      KK = KK - NT + KSPAN
C      IF (KK .LE. KSPNN) GO TO 730
C      C2 = C1 - (CD * C1 + SD * S1)
C      S1 = S1 + (SD * C1 - CD * S1)
C      C1 = 0.5 / (C2**2 + S1**2) + 0.5
C      S1 = C1 * S1
C      C2 = C1 * C2
C      KK = KK - KSPNN + JC
C      IF (KK .LE. KSPAN) GO TO 720
C      KK = KK - KSPAN + JC + INC
C      IF (KK .LE. JC + JC) GO TO 710
C      CC TO 100

```

```

CFFFT5710
CFFFT5720
CFFFT5730
CFFFT5740
CFFFT5750
CFFFT5760
CFFFT5770
CFFFT5780
CFFFT5790
CFFFT5800
CFFFT5810
CFFFT5820
CFFFT5830
CFFFT5840
CFFFT5850
CFFFT5860
CFFFT5870
CFFFT5880
CFFFT5890
CFFFT5900
CFFFT5910
CFFFT5920
CFFFT5930
CFFFT5940
CFFFT5950
CFFFT5960
CFFFT5970
CFFFT5980
CFFFT5990
CFFFT6000
CFFFT6010
CFFFT6020
CFFFT6030
CFFFT6040
CFFFT6050
CFFFT6060
CFFFT6070
CFFFT6080
CFFFT6090
CFFFT6100
CFFFT6110
CFFFT6120
CFFFT6130
CFFFT6140
CFFFT6150
CFFFT6160
CFFFT6170
CFFFT6180

```



```

C      PERMUTE RESULTS TO NORMAL ORDER IN TWO STAGES:
C      PERMUTATION FOR SQUARE FACTORS OF N
C
C      800 NP(1) = KS
C      IF (KT .EQ. 0) GO TO 890
C
C      K = KT + KT + 1
C      IF (M .LT. K) K = K - 1
C
C      J = 1
C      NP(K+1) = JC
C
C      810 NP(J+1) = NP(J)/NFAC(J)
C      NP(K) = NP(K+1) * NFAC(J)
C
C      J = J + 1
C      K = K - 1
C      IF (J .LT. K) GO TO 810
C
C      K3 = NP(K+1)
C      KSPAN = NP(2)
C      KK = JC + 1
C      K2 = KSPAN + 1
C
C      J = 1
C      IF (N .NE. NTOT) GO TO 850
C
C      PERMUTATION FOR SINGE-VARIATE TRANSFORM
C
C      820 AK = A(KK)
C      A(KK) = A(K2)
C      A(K2) = AK
C
C      BK = B(KK)
C      B(KK) = B(K2)
C      B(K2) = BK
C
C      KK = KK + INC
C      K2 = KSPAN + K2
C      IF (K2 .LT. KS) GO TO 820
C
C      830 K2 = K2 - NP(J)
C      J = J + 1
C      K2 = NP(J+1) + K2
C      IF (K2 .GT. NP(J)) GO TO 830
C      J = 1

```

```

CFFT6190
CFFT6200
CFFT6210
CFFT6220
CFFT6230
CFFT6240
CFFT6250
CFFT6260
CFFT6270
CFFT6280
CFFT6290
CFFT6300
CFFT6310
CFFT6320
CFFT6330
CFFT6340
CFFT6350
CFFT6360
CFFT6370
CFFT6380
CFFT6390
CFFT6400
CFFT6410
CFFT6420
CFFT6430
CFFT6440
CFFT6450
CFFT6460
CFFT6470
CFFT6480
CFFT6490
CFFT6500
CFFT6510
CFFT6520
CFFT6530
CFFT6540
CFFT6550
CFFT6560
CFFT6570
CFFT6580
CFFT6590
CFFT6600
CFFT6610
CFFT6620
CFFT6630
CFFT6640
CFFT6650
CFFT6660

```



```

      840 IF (KK .LT. K2) GO TO 820
      C
      KK = KK + INC
      K2 = KSPAN + K2
      IF (K2 .LT. KS) GO TO 840
      C
      IF (KK .LT. KS) GO TO 830
      C
      JC = K3
      GC TO 850
      C
      PERMUTATION FOR MULTIVARIATE TRANSFORM
      C
      850 K = KK + JC
      C
      860 AK = A(KK)
      A(KK) = A(K2)
      A(K2) = AK
      C
      BK = B(KK)
      B(KK) = B(K2)
      B(K2) = BK
      C
      KK = KK + INC
      K2 = K2 + INC
      IF (KK .LT. K) GO TO 860
      C
      KK = KK + KS - JC
      K2 = K2 + KS - JC
      IF (KK .LT. NT) GO TO 850
      C
      K2 = K2 - NT + KSPAN
      KK = KK - NT + JC
      IF (K2 .LT. KS) GO TO 850
      C
      870 K2 = K2 - NP(J)
      J = J + 1
      C
      K2 = NP(J+1) + K2
      IF (K2 .GT. NP(J)) GO TO 870
      J = 1
      C
      880 IF (KK .LT. K2) GO TO 850
      KK = KK + JC
      K2 = KSPAN + K2
      C
      IF (K2 .LT. KS) GO TO 880
      C

```

```

CFFI6670
CFFI6680
CFFI6690
CFFI6700
CFFI6710
CFFI6720
CFFI6730
CFFI6740
CFFI6750
CFFI6760
CFFI6770
CFFI6780
CFFI6790
CFFI6800
CFFI6810
CFFI6820
CFFI6830
CFFI6840
CFFI6850
CFFI6860
CFFI6870
CFFI6880
CFFI6890
CFFI6900
CFFI6910
CFFI6920
CFFI6930
CFFI6940
CFFI6950
CFFI6960
CFFI6970
CFFI6980
CFFI6990
CFFI7000
CFFI7010
CFFI7020
CFFI7030
CFFI7040
CFFI7050
CFFI7060
CFFI7070
CFFI7080
CFFI7090
CFFI7100
CFFI7110
CFFI7120
CFFI7130
CFFI7140

```



```

      IF (KK .LT. KS) GO TO 870
      JC = K3
C 850 IF (2 * KT + 1 .GE. M) RETURN
C      KSPNN = NP(KT+1)
C      PERMUTATION FOR SQUARE-FREE FACTORS CF N.
C      J = M - KT
      NFAC(J+1) = 1
C 900 NFAC(J) = NFAC(J) * NFAC(J+1)
      J = J - 1
      IF (J .NE. KT) GO TO 900
C      KT = KT + 1
      NN = NFAC(KT) - 1
      IF (NN .GT. MAXP) GO TO 998
C      JJ = 0
      J = 0
      GC TO 906
C 902 JJ = JJ + K2
      K2 = KK
      K = K + 1
      KK = NFAC(K)
C 904 JJ = KK + JJ
      IF (JJ .GE. K2) GO TO 902
C      NP(J) = JJ
C 906 K2 = NFAC(KT)
      K = KT + 1
      KK = NFAC(K)
C      J = J + 1
      IF (J .LE. NN) GO TO 904
C      DETERMINE PERMUTATION CYCLES CF LENGTH .GT. 1
C      J = 0
      GO TO 914
C 910 K = KK
      KK = NP(K)

```

```

CFFT7150
CFFT7160
CFFT7170
CFFT7180
CFFT7190
CFFT7200
CFFT7210
CFFT7220
CFFT7230
CFFT7240
CFFT7250
CFFT7260
CFFT7270
CFFT7280
CFFT7290
CFFT7300
CFFT7310
CFFT7320
CFFT7330
CFFT7340
CFFT7350
CFFT7360
CFFT7370
CFFT7380
CFFT7390
CFFT7400
CFFT7410
CFFT7420
CFFT7430
CFFT7440
CFFT7450
CFFT7460
CFFT7470
CFFT7480
CFFT7490
CFFT7500
CFFT7510
CFFT7520
CFFT7530
CFFT7540
CFFT7550
CFFT7560
CFFT7570
CFFT7580
CFFT7590
CFFT7600
CFFT7610
CFFT7620

```



```

      NP(K) = -KK
      IF (KK.NE. J) GO TO 910
      K 3 = KK
C 914 J = J + 1
      KK = NP(J)
      IF (KK.LT. 0) GO TO 914
C      IF (KK.NE. J) GO TO 910
C
      NP(J) = -J
      IF (J.NE. NN) GO TO 914
      MAXF = INC * MAXF
C      REORDER A AND B, FOLLOWING PERMUTATION CYCLES.
C      GO TO 950
C 924 J = J - 1
      IF (NP(J).LT. 0) GO TO 924
      JJ = JC
C 926 KSPAN = JJ
      IF (JJ.GT. MAXF) KSPAN = MAXF
C      JJ = JJ - KSPAN
      K = NP(J)
      KK = JC * K + II + JJ
      K1 = KK + KSPAN
      K2 = 0
C 928 K2 = K2 + 1
      AT(K2) = A(K1)
      BT(K2) = B(K1)
C      K1 = K1 - INC
      IF (K1.NE. KK) GO TO 928
C 932 K1 = KK + KSPAN
      K2 = K1 - JC * (K+NP(K))
      K = -NP(K)
C 936 A(K1) = A(K2)
      B(K1) = B(K2)
C      K1 = K1 - INC
      K2 = K2 - INC
      IF (K1.NE. KK) GO TO 936

```

```

CFFT7630
CFFT7640
CFFT7650
CFFT7660
CFFT7670
CFFT7680
CFFT7690
CFFT7700
CFFT7710
CFFT7720
CFFT7730
CFFT7740
CFFT7750
CFFT7760
CFFT7770
CFFT7780
CFFT7790
CFFT7800
CFFT7810
CFFT7820
CFFT7830
CFFT7840
CFFT7850
CFFT7860
CFFT7870
CFFT7880
CFFT7890
CFFT7900
CFFT7910
CFFT7920
CFFT7930
CFFT7940
CFFT7950
CFFT7960
CFFT7970
CFFT7980
CFFT7990
CFFT8000
CFFT8010
CFFT8020
CFFT8030
CFFT8040
CFFT8050
CFFT8060
CFFT8070
CFFT8080
CFFT8090
CFFT8100

```



```

C      KK = K2
C      IF (K .NE. J) GO TO 932
C
C      K1 = KK + KSPAN
C      K2 = 0
C
C      940 K2 = K2 + 1
C      A(K1) = AT(K2)
C      B(K1) = BT(K2)
C
C      K1 = K1 + INC
C      IF (K1 .NE. KK) GO TO 940
C
C      IF (JJ .NE. 0) GO TO 926
C
C      IF (J .NE. 1) GO TO 924
C
C      950 J = K3 + 1
C      NT = NT - KSPNN
C      II = NT - INC + 1
C      IF (NT .GE. 0) GO TO 924
C
C      RETURN
C
C      ERROR TERMINATION: INS
C
C      998 ISN = 0
C      STOP 999
C      END

```



```

*EVE000430
*EVE000440
*EVE000450
*EVE000460
*EVE000470
*EVE000480
*EVE000490
*EVE000500
*EVE000510
*EVE000520
*EVE000530
*EVE000540
*EVE000550
*EVE000560
*EVE000570
*EVE000580
*EVE000590
*EVE000600
*EVE000610
*EVE000620
*EVE000630
*EVE000640
*EVE000650
*EVE000660
*EVE000670
*EVE000680
*EVE000690
*EVE000700
*EVE000710
*EVE000720
*EVE000730
*EVE000740
*EVE000750
*EVE000760
*EVE000770
*EVE000780
*EVE000790
*EVE000800
*EVE000810
*EVE000820
*EVE000830
*EVE000840
*EVE000850
*EVE000860
*EVE000870
*EVE000880
*EVE000890
*EVE000900

```

```

MICRCNS. AND XLAMDA CN THIRD DATA CARD IN (2F10.5) FORMAT
RHOINF AND XLAMDA CN THIRD DATA CARD IN (2F10.5) FORMAT
MODE MODE=1 REFRACTIVE INDEX SUPPLIED THROUGH SUBRCUTINE
AND RECOMPUTES THE PROGRAM GENERATES FRINGE DATA
AND RECOMPUTES THE REFRACTIVE INDEX FROM
THE GENERATE INDEX SUPPLIED AT GRID POINTS
BY INPUT DATA. PROGRAM PROCEEDS AS IN MODE 1
MODE=2 REFRACTIVE INDEX SUPPLIED, PROGRAM GENERATES
FRINGE DATA.
MODE=3 DENSITY FIELD.
MODE=4 SAME AS MODE=3 EXCEPT FRINGE DATA IS RECOM-
PUTED AS PER DATA POINTS
NP NUMBER OF EQUALLY SPACED
NT NUMBER OF VIEWS SUPPLIED
KSYM SYMMETRY OF FIELD 0-4 AXIS OF SYMMETRY
4 -98 DATA REPEATS EVERY KSYM
CEGREES. FIELD
99 AXIS SYMMETRIC FIELD
RMAX RADIUS OF CIRCULAR REGION IN CENTIMETERS
FILTER = (0.-1.) DETERMINES SPAN OVER WHICH AVERAGING OCCURS
THE INFORMATION ON THE FOURTH DATA CARD (411C,2F10.5).
X(I) VECTOR OF GRID PCINTS ALONG THETA = 0 DEGREES
X(1)=-RMAX X(NP)=+RMAX
Y(J) VECTOR OF GRID PCINTS ALONG THETA=90 DEGREES
Y(1)=-RMAX Y(NP)=+RMAX
A(I,J) DENSITY OR REFRACTIVE INDEX AT THE PCINT X(I),Y(J).
RB(I,J) VECTOR CF POINTS ON THE PLOGRAPHIC PLATE RB(1)=-2 RMAX
RB(2,NP)=2 RMAX. GRID SPACING OF RAYS. DR=2*RMAX/(NP-1)
DR SPACING OF VIEWING ANGLES IN DEGREES
TH(K) VECTOR CF SHIFT INFORMATION AT THE POINT (RB(I),TH(K)).
B(I,K) FRINGED INTC BB(I,K). THE VALUE CF THE INSIDE
B(I,K) IS COPIED INTO STORED IN B(I,K).
INTEGRATION IS THEN STORED IN B(I,K).
DASYM(K) SYMMETRY OF DATA (B(I,K). 0 NC SYMMETRY
1 DATA SYMETRIC ABOUT RB=0.
IF DASYM = 1.0 ONLY (NP+1)/2 DATA POINTS SHOULD BE FURNISHED.
BD(L) IS A VECTOR USED BY THE PROGRAM.
FOR MODE=1 OR MODE=2 THE FIFTH DATA CARD IS THE VECTOR
TH(K) IN (8F10.5) FORMAT
FOR MODE 2 OPERATION THE REFRACTIVE INDEX FOLLOWS IN 8F10.5
FOR MODE 3 AND MODE=4 OPERATION, THE FIFTH DATA CARD IS
TH(1) AND DASYM(1) IN (2F10.5) FORMAT. THIS IS FOLLOWED
BY THE FRINGE INFORMATION FOR THAT VIEW. (B(1,1) ETC UNTIL
ALL VIEWS AND FRINGE SHIFT HAS BEEN SUPPLIED
IF AXIS OF SYMMETRY EXISTS, THETA=0. MUST CORRESPOND TO ONE OF
THE AXIS OF SYMMETRY.

```

CC

C

```

*****REAL*8, IT(12), LAB, ITSUB(12), REFRAC TI, 'VE INDEX', 'DENSITY', 'IN ME
100      THET, 'A= ODEG', 'THET', 'A= 45DEG', 'THET', 'A=--4
101      15DEG, /
102      DIMENSION X(151), Y(151), A(151,151), B(151,20), CC(36),
103      188(301,20), RB(301), DASYM(20), SS(36), CC(36)
104      INTEGER CLOCK(6)
105      DATA C1, C2, C3, C4 / .252857, 1.54285, .192857, 1.54285 /, LAB, '
106      FCRMAT(4110,2F10.5)
107      FCRMAT('O', T20, 'MODE NUM PTS NUM VIEWS KSYM RADIUS
108      1 GRID SPACING FILTER')
109      FCRMAT('O', T17, 4110, 3F10.5)
110      FCRMAT(8F10.5)
111      FCRMAT('O', T7, 20F6.1 / /)
112      FCRMAT('O', F5.2, 20F6.2)
113      FCRMAT('O', T9, 'MODE 1', T26, 'MODE 3', T45, 'VALUE', T9, 'GIVEN COMP
114      DENSITY', T47, 'OF', 'RADIUS REFRAC REFRACTI, 'VE INDEX', 'DENSITY', 'IN ME
115      1 INSIDE', 'CM INDEX INDEX MG/CC SHIFT FIELD INTEGRAL,
116      2 //)
117      FCRMAT('O', T20, 'RHGINF =', F7.5, 'MG/CC LAMDA=', F7.5, ' MICRONS')
118      FCRMAT('O', T7, 21F6.2 / /)
119      FCRMAT('O', F5.2, 1X, 21F6.2)
120      FCRMAT(6A8)
121      1 X AXIS(THETA=90 DEGREES) VERTICAL', T40,
122      FCRMAT('O', T40, 'DENSITY FIELD IN MG/CC FOLLOWS')
123      FCRMAT('O', T40, 'INDEX OF REFRACTICN FOLLOWS')
124      FCRMAT('O', T40, 'THE EXPANDED FRINGE SHIFT INFORMATION IS AS FOLLOWS')
125      FCRMAT('O', T40, 'THE VALUE OF THE INSIDE INTEGRATION IS AS FOLLOWS')
126      FCRMAT(10F7.4)
127      READ(1,112) (IT(I), I=1,12)
128      READ(1,103) RHGINF, XLAMD
129      READ(1,100) MODE, NP, NT, KSYM, RMAX, FILTER
130      WRITE(3,108) RHGINF, XLAMD
131      FNP=FLOAT(NP)
132      DR=2.*RMAX/(FNP-1)
133      WRITE(8,101)
134      WRITE(8,102) MODE, NP, NT, KSYM, RMAX, DR, FILTER
135      N=(NP+1)/2
136      NPL=(NP-1)/2
137      NPP=2*NPL
138      MAX=NP+NPL
139      RM2=RMAX**2
140      FNP5=3*NPL-2
141      FNP5=FLCAT(NP5)
142      NPM1=NP-1
143      FT2=FILTER*FILTER

```



```

C*****ZERO MATRICES AND SET GRID *****
C
C
DO 2 I=1,NP
DO 1 J=1,NP
1 A(I,J)=0.0
2 B(I,K)=0.0
2 B(I,K)=0.0
2 X(I)=RMAX
Y(I)=X(I)
DC 3 I=2,NP
X(I)=X(I-1)+DR
3 Y(I)=X(I)
C*****READ VIEWING ANGLES AND SET SIN AND COSINE FOR MODE=1,2*****
C
4 READ(1,103) (TH(K),K=1,NT)
DC 5 K=1,NT
THETA=TH(K)/57.296
CC(K)=CCS(THETA)
5 SS(K)=SIN(THETA)
7 IF(KSYM.EQ.99) GO TO 13
C*****SET REFRACTIVE INDEX AND WRITE SAME FOR NCCE CNE OPERATION*****
C
C
DC 8 I=1,NP
DO 8 J=1,NP
XI=X(I)
YJ=Y(J)
CALL INPUT(XI,YJ,VAL)
8 5 A(I,J)=VAL
5 WRITE(8,115)
WRITE(8,113)
K=1
K21=21
11 WRITE(8,106) (X(I),I=K,K21)
WRITE(8,110)
DC 12 I=1,NP
NN=NP-I+1
12 WRITE(8,111) Y(NN),A(J,NN),J=K,K21)
IF(K21.EQ.NP) GO TO 15
K=K21+1
K21=K21+21
IF(K21.GT.NP) K21=NP
GO TO 11
C*****
C*****SET REFRACTIVE INDEX FOR AXISYMETRIC CASE*****
C
C
C

```

```

VE01390
VE01400
VE01410
VE01420
VE01430
VE01440
VE01450
VE01460
VE01470
VE01480
VE01490
VE01500
VE01510
VE01520
VE01530
VE01540
VE01550
VE01560
VE01570
VE01580
VE01590
VE01600
VE01610
VE01620
VE01630
VE01640
VE01650
VE01660
VE01670
VE01680
VE01690
VE01700
VE01710
VE01720
VE01730
VE01740
VE01750
VE01760
VE01770
VE01780
VE01790
VE01800
VE01810
VE01820
VE01830
VE01840
VE01850
VE01860

```



```

38 BB(K,I)=-3.*Q2+RB(K)*(3.*Q2+4.*C1/3.+RB(K)*(-Q2/1.5-C1/2.25))
DC 381 I=1,NT
DC 382 J=1,NPP
WRITE(3,1001) BB(J,I),J,I
1001 FCRMAT(F10.5,2I10)
382 CCNTINUE
381 CCNTINUE
C *****
C *****
C *****
C *****CALCULATE VALUE OF INSIDE INTEGRAL *****
C *****
DC 43 I=1,NT
DC 43 J=1,NP
M=NPL+J
BD(1)=0.
CC 39 K=1,MAX
MKP=M+K
MKM=M-K
IF(MKP.GT.NPP) MKP=NPP
IF(MKM.LT.1) MKM=1
K1=K**2
39 BC(K+1)=(BB(MKP,I)+BB(MKM,I)-2.*BB(M,I))/(FLCAT(K1)*CR)
IF(J.GT.20) GO TO 391
WRITE(3,1002) (BD(L),L=1,98)
1002 FCRMAT(10F8.3)
391 CCNTINUE
VAL=0.
K1=1
40 K2=K1+6
IF(K2.GT.MAX) GO TO 41
CCIES SIXTH ORDER QUADATURE FORMULA*****
VAL=VAL+C1*(BD(K1)+BD(K2))+C2*(BD(K1+1)+BD(K2-1))+C3*(BD(K1+2)+BD(K2-2))+C4*BD(K1+3)
K1=K2
GO TO 40
41 SUM=0.
CCNTIRIBUTION OF LAST TERMS
DO 42 K=K1,MAX
SUM=SUM+BD(K)+BD(K+1)
42 SUM=COTES PLUS LAST TERMS PLUS INTEGRATION FROM 2 RMAX TO INFINITY
B(J,I)= VAL+SUM/2.-.666667*BB(M,I)/RMAX
WRITE(3,1001) B(J,I),J,I
43 CCNTINUE
IF(KSYM.LT.99) GO TO 48
C *****

```

```

EVE02350
EVE02360
EVE02370
EVE02380
EVE02390
EVE02400
EVE02410
EVE02420
EVE02430
EVE02440
EVE02450
EVE02460
EVE02470
EVE02500
EVE02510
EVE02520
EVE02530
EVE02540
EVE02550
EVE02560
EVE02570
EVE02580
EVE02590
EVE02600
EVE02610
EVE02620
EVE02630
EVE02640
EVE02650
EVE02660
EVE02670
EVE02680
EVE02690
EVE02700
EVE02710
EVE02720
EVE02730
EVE02740
EVE02750
EVE02760
EVE02770
EVE02780
EVE02790
EVE02800
EVE02810
EVE02820
EVE02830
EVE02840

```



```

C REFRACTIVE INDEX SUPPLIED*****
GC TO 75
CCCONTINUE
48 M=NT+1
IF(KSYM.EQ.0) GO TO 51
IF(KSYM.GT.4) GO TO 53
C*****GENERATE ADDITIONAL DATA DEPENDING ON SYMETRY OF FIELD*****
C
C DT=TH(2)-TH(1)
NTP=NT
DO 50 J=1,KSYM
K=J*NT
DO 49 I=1,NTP
KK=K+I
TH(KK)=TH(KK-1)+DT
KM=K-I+1
DC 49 L=1,NP
45 B(L,KK)=B(L,KM)
50 NTP=2*NTP
M=KK+1
C*****GENERATE DATA FOR 180 DEGREE VIEW*****
C
C 51 TH(M)=TH(1)+180.
DC 52 I=1,NP
K=(NP-I+1)
52 B(K,M)=B(I,1)
C*****
C
C GC TO 55
C*****GENERATE ADDITIONAL DATA FOR REPEATING DATA*****
C
C 53 M=180/KSYM+1
DC 54 I=2,M
TH(I)=TH(I-1)+FLOAT(KSYM)
DC 54 J=1,NP
54 B(J,I)=B(J,I-1)
55 CCNTINUE
C*****
C
C*****INTEGRATE ON THETA FOR ASYMETRIC FIELD*****
C
C

```

```

EVE03330
EVE03340
EVE03350
EVE03380
EVE03390
EVE03400
EVE03410
EVE03420
EVE03430
EVE03440
EVE03450
EVE03460
EVE03470
EVE03480
EVE03490
EVE03500
EVE03510
EVE03520
EVE03530
EVE03540
EVE03550
EVE03560
EVE03570
EVE03580
EVE03590
EVE03600
EVE03610
EVE03620
EVE03630
EVE03640
EVE03650
EVE03660
EVE03670
EVE03680
EVE03690
EVE03700
EVE03710
EVE03720
EVE03730
EVE03740
EVE03750
EVE03760
EVE03770
EVE03780
EVE03790
EVE03800
EVE03810
EVE03820

```



```

MD=M-1/(2.*3.1416*FLOAT(MD))
DEL=-1
DO 56 I=1,M
  CC(I)=COS(TH(I)/57.296)
  SS(I)=SIN(TH(I)/57.296)
56 DO 61 LL=1,NP
  J=NP+1-LL
  DC 60 I=1,NP
  A(I,J)=0.
  DC 58 K=1,M
  R=Y(J)*CC(K)-X(I)*SS(K)
  NN=(R+RMAX+DR)/DR
  IF(NN*GE.NP) GO TO 60
  IF(NN*LT.1) GO TO 60
  LP1=NN+1
  LM1=NN-1
  IF(LP2*GT.NP) LP2=NP
  IF(LM1*LT.1) LM1=1
  P=(R-X(NN))/DR
  COF3=.1666666*(B(LP2,K)-B(LP1,K))-5*(B(LP1,K)-B(NN,K))
  COF2=-.5*(B(LP1,K)+B(LP2,K))-3333333*B(LP1,K)-.5*B(NN,K)
  P2=P*P
C*****AMOUNT OF FILTERING DEPENDS ON FT2=FILTER*FILTER*****
58 BD(K)=P*(P2+FT2)*COF3+(P2+.666666*FT2)*COF2+P*COF1+B(NN,K)
C INTEGRATE OVER THETA USING TRAPEZOIDAL INTEGRATION*****
  VAL=0.0
  DO 59 L=2,M
    VAL=VAL+BD(L)+BD(L-1)
59 A(I,J)=VAL*DEL/2.
C*****
60 CC CONTINUE
61 CC CONTINUE
C*****
C*****
NPN=NP+NPL
IF(MODE*LT.4) GO TO 63
63 IF(MODE*LT.3) GO TO 65
C*****CHANGE REFRACTIVE INDEX FIELD TO DENSITY FIELD*****
DC 64 I=1,NP
DC 64 J=1,NP
64 A(I,J)=RHOINF+.4443*XLAMD*A(I,J)
C*****
C*****

```

```

EVE03830
EVE03840
EVE03850
EVE03860
EVE03870
EVE03880
EVE03890
EVE03900
EVE03910
EVE03920
EVE03930
EVE03940
EVE03950
EVE03960
EVE03970
EVE03980
EVE03990
EVE04000
EVE04010
EVE04020
EVE04030
EVE04040
EVE04050
EVE04060
EVE04070
EVE04080
EVE04090
EVE04100
EVE04110
EVE04120
EVE04130
EVE04140
EVE04150
EVE04160
EVE04170
EVE04180
EVE04190
EVE04200
EVE04210
EVE04220
EVE04230
EVE04240
EVE04250
EVE04260
EVE04270
EVE04280
EVE04290
EVE04300

```



```

WRITE(8,114)
GO TO 66
65 WRITE(8,115)
66 WRITE(8,113)
C
C*****WRITE REFRACTIVE INDEX OR DENSITY FIELD*****
C
K=1
K21=21
WRITE(8,106) (X(I),I=K,K21)
67 WRITE(8,110) (X(I),I=1,NP)
DC 68 I=1,NP
NN=NP-I+1
68 WRITE(8,111) Y(NN), (A(J,NN),J=K,K21)
IF(K21.EQ.NP) GO TO 69
K=K21+1
K21=K21+21
IF(K21.GT.NP) K21=NP
69 WRITE(8,116)
C
C*****WRITE FRINGE SHIFT INFORMATION*****
C
WRITE(8,104) (TH(K),K=1,NT)
CC 70 I=N,NPN
70 WRITE(8,105) RB(I), (BB(I,J),J=1,NT)
C
WRITE(8,115)
WRITE(8,104) (TH(K),K=1,NT)
DO 700 J=1,NT
WRITE(8,103) TH(J)
WRITE(8,103) (BB(I,J),I=N,NPN)
700 CCNTINUE
C
WRITE(2,112) (IT(I),I=1,12)
WRITE(2,103) RHOINF,XLAM0
WRITE(2,100) MODE,NP,NT,KSYP,RMAX,FILTER
DO 710 J=1,NT
WRITE(2,103) TH(J)
WRITE(2,103) (BB(I,J),I=N,NPN)
710 CCNTINUE
C
WRITE(8,117)
WRITE(8,104) (TH(K),K=1,M)
DC 71 I=1,NP

```


APPENDIX F. ALTERNATE PROGRAMS DESIGNED TO CALCULATE THE INSIDE INTEGRAL

APPENDIX F.1 JONES1--USING CONVOLUTION VALUES OBTAINED NUMERICALLY

See Appendix F.2 for expanded fringe shift information used as input fringe data for $-1.5 \leq R \leq 1.5$

```

DIMENSION X(513),Y(513),Z(513) ,XD(513),YD(513),B(513)
N=512
PY=3.141593
R=12.0
FA=N
DR=2.*R/FN
C*****LIMITS FOR READING DATA AND PRINTING OUTPUTS*****
INTE=1
INTE=65
INTPRB=256
INTPRE=322
NPL=N+1
DO 21 I=1,NPL
  Y(I)=0.0
  21 CCNTINUE
  301 READ (1,301) (Y(M),M=INTB,INTE)
  301 FORMAT(F10.5)
  DO 22 I=1,NPL
    B(I)=0.0
    IF (I.LE. INTPRB) GO TO 22
    IF (I.GE. INTPRE) GO TO 22
    C*****PRINT CHECK FOR PROPER INPUT OF FRINGE DATA*****
    WRITE (4,101) Y(I),B(I),I
    22 CCNTINUE
  DO 5 K=1,NPL
    C=-R+DR*(K-1)
    IF (C.EQ.0.0) GO TO 6
    X(K)=1./C
    GO TO 7
  6 X(K)=0.
  7 CCNTINUE
  IF (K.LE. INTPRB) GO TO 5
  IF (K.GE. INTPRE) GO TO 5
  C*****PRINT CHECK FOR PROPER INPUT OF 1/R VECTOR*****
  WRITE(4,201) X(K),Y(K),K,C
  201 FORMAT(2F10.5,I10,F10.5)
  5 CCNTINUE
  DO 10 I=1,N
    Z(I)=0.0
    DO 9 J=1,I
      Z(I)=Z(I)+X(J)*Y(I+1-J)
    
```



```

9 CONTINUE
  Z(I)=Z(I)*DR
  IF (I.LE.INTPRB) GO TO 10
  IF (I.LE.INTPRE) GO TO 10
  PRINT (I, 'CHECK OF VALUE OF NUMERICAL CONVOLUTION*****')
  C****
  101 WRITE(4,101) Y(I), Z(I), I
  1C FORMAT(2F10.5, I10)
  CONTINUE
  CALL CFFT2(Z,B,N,N,N,-1)
  DO 15 I=1,N
    Z(I)=Z(I)/FN
    P(I)=B(I)/FN
    T=2.*PY*(I-1.)/FN
    XD(I)=-SIN(T)*B(I)/DR
    YD(I)=SIN(T)*Z(I)/DR
    IF (I.LE.INTPRB) GO TO 15
    IF (I.LE.INTPRE) GO TO 15
    PRINT (I, 'CHECK OF FOURIER COEFFICIENTS OF CONVOLUTION AND THEIR
    C****
    C****
    501 WRITE(4,501) Z(I), B(I), I, XD(I), YD(I)
    15 FORMAT(2F10.5, I10, 2F10.5)
    CONTINUE
    CALL CFFT2(XD,YD,N,N,N,1)
    DO 30 J=1,N
      WRITE(4,101) XD(J), YD(J), J
      REAL AND IMAGINARY COEFFICIENTS OF THE INSIDE
      C****
      C****
      30 CONTINUE
      DO 35 I=257,321
        C****
        C****
        601 WRITE(3,601) XD(I)
        35 FORMAT (F10.5)
        CONTINUE
        STOP
      END

```

```

HAL000430
HAL000440
HAL000450
HAL000460
HAL000470
HAL000480
HAL000490
HAL000500
HAL000510
HAL000520
HAL000530
HAL000540
HAL000550
HAL000560
HAL000570
HAL000580
HAL000590
HAL000600
HAL000610
HAL000620
HAL000630
HAL000640
HAL000650
HAL000660
HAL000670
HAL000680
HAL000690
HAL000700
HAL000710
HAL000720
HAL000730
HAL000740
HAL000750
HAL000760
HAL000770

```


APPENDIX F.2. JONES2--USING CONVOLUTION VALUES OBTAINED WITH FFT METHODS

See Appendix F.3 for expanded fringe shift information used as input fringe data for

$1.5 \leq R \leq 1.5$

DIMENSION A(513), B(513), D(513), FA(513), FB(513), FX(513)
 DIMENSION FY(513), XC(513), YC(513), X(513), Y(513), XD(513), YD(513)
 PY=3.141592653

R=12.0

N=512

FN=N

DR=2.*R/FN

INTB=1

INTE=65

INTPRB=256

INTPRE=322

NPI=N+1

C INITIALIZE VECTORS TO ZERO

DO 110 I=1,NPI

A(I)=0.0

B(I)=0.0

X(I)=0.0

Y(I)=0.0

110 CONTINUE

C FRINGE DATA STORED IN A(I) FOR I FROM INTB-INTE.

DO 120 I=INTB,INTE

READ (1,1001) A(I)

1001 FORMAT (F10.5)

120 CONTINUE

C 1/2 STORED IN X(I) FOR I FROM 1,N.

DO 130 I=1,N

C=-R+DR*(I-1)

IF(C.EQ.0.00) GO TO 9

X(I)=1./C

GO TO 11

9 X(I)=0.0

11 CONTINUE

IF (I.LE. INTPRB) GO TO 130

IF (I.GE. INTPRE) GO TO 130

C PRINTOUT CHECK TO ENSURE DATA INPUTTED CORRECTLY.

WRITE (4,101) X(I),Y(I),I,A(I),B(I),C

101 FORMAT (2F10.5,110,3F10.5)

130 CONTINUE

C TAKING FFT OF INPUT DATA

C REAL COEFFICIENTS RETURNED AND PLACED IN FA AND FX.

C IMAGINARY COEFFICIENTS RETURNED AND STORED IN FB AND FY.

CALL CFFT2(X,Y,N,N,-1)

HAC000010
 HAC000020
 HAC000030
 HAC000040
 HAC000050
 HAC000060
 HAC000070
 HAC000080
 HAC000090
 HAC000100
 HAC000110
 HAC000120
 HAC000130
 HAC000140
 HAC000150
 HAC000160
 HAC000170
 HAC000180
 HAC000190
 HAC000200
 HAC000210
 HAC000220
 HAC000230
 HAC000240
 HAC000250
 HAC000260
 HAC000270
 HAC000280
 HAC000290
 HAC000300
 HAC000310
 HAC000320
 HAC000330
 HAC000340
 HAC000350
 HAC000360
 HAC000370
 HAC000380
 HAC000390
 HAC000400
 HAC000410
 HAC000420


```

CALL CFFT2(A,B,N,N,N,-1)
DC 20 J=1,N
FX(J)=X(J)/FN
FY(J)=Y(J)/FN
FA(J)=A(J)/FN
FB(J)=B(J)/FN
IF (J.LE.INTPRB) GO TO 20
IF (J.GE.INTPRE) GO TO 20
IF (J.EQ.INTPRB) GO TO 20
C PRINT CHECK OF FOURIER COEFFICIENTS CF FRINGE DATA AND 1/C.
201 WRITE (4,201) FX(J),FY(J),J,FA(J),FB(J)
20 FCRMAT (2F10.5,I10,2F10.5)
20 CCNTINUE=1,N
DC 21 J=1,N
XC(J)=FX(J)*FA(J)-FY(J)*FB(J)
YC(J)=FY(J)*FA(J)+FX(J)*FB(J)
XC(J)=XC(J)*2.*R
YC(J)=YC(J)*2.*R
IF (J.LE.INTPRB) GO TO 21
IF (J.GE.INTPRE) GO TO 21
IF (J.EQ.INTPRB) GO TO 21
C PRINT CHECK OF FOURIER COEFFICIENTS OF CONVOLUTION.
301 WRITE (4,301) XC(J),YC(J),J
301 FCRMAT (2F10.5,I10)
301 CCNTINUE=1,N
DC 22 J=1,N
T=2.*PY*(J-1)/FN
XC(J)=-SIN(T)*YC(J)/DR
YC(J)=SIN(T)*XC(J)/DR
IF (J.LE.INTPRB) GO TO 22
IF (J.GE.INTPRE) GO TO 22
IF (J.EQ.INTPRB) GO TO 22
C PRINT CHECK OF DIFFERENTIATION OF FOURIER COEFFICIENTS OF CONVOLUTION
401 WRITE (4,401) XD(J),YD(J),J
401 FCRMAT (2F10.5,I10)
401 CCNTINUE=1,N
DC 30 K=1,N
CALL CFFT2 (XD,YD,N,N,N,1)
DO 30 K=1,N
WRITE (4,301) XD(K),YD(K),K
C PRINT OUT CF VALUES OF INSIDE INTEGRAL.
C FIRST, Q. POINTS ARE INVALID.
30 CCNTINUE=1,N
DC 35 I=257,321
WRITE (3,601) XD(I)
601 FCRMAT (F10.5)
601 CCNTINUE=1,N
DC 35 I=257,321
CALL CFFT2 (XC,YC,N,N,N,1)
C CBTAINING THE INVERSE DFT OF FOUR. COEFF. OF CONVOLUTION.
DC 40 L=1,N
IF (L.LE.INTPRE) GO TO 40
IF (L.GE.INTPRE) GO TO 40

```

HAC00430
HAC00440
HAC00450
HAC00460
HAC00470
HAC00480
HAC00490
HAC00500
HAC00510
HAC00520
HAC00530
HAC00540
HAC00550
HAC00560
HAC00570
HAC00580
HAC00590
HAC00600
HAC00610
HAC00620
HAC00630
HAC00640
HAC00650
HAC00660
HAC00670
HAC00680
HAC00690
HAC00700
HAC00710
HAC00720
HAC00730
HAC00740
HAC00750
HAC00760
HAC00770
HAC00780
HAC00790
HAC00800
HAC00810
HAC00820
HAC00830
HAC00840
HAC00850
HAC00860
HAC00870
HAC00880
HAC00890
HAC00900

HAC00910
HAC00920
HAC00930
HAC00940
HAC00950

C WRITE (4,401) XC(L),YC(L),L
 REAL COEFF: ARE IN FIRST COLUMN, IMAG. COEF. IN SECOND COL.
4C CONTINUE
 STOP
 END

APPENDIX F.3. EXPANDED FRINGE SHIFT INFORMATION USED IN JONES1 AND JONES2

This data was obtained from Van Houten's computer program for MODE ONE operation using control cards as explained in Van Houten's thesis [17] for the asymmetric Gaussian case with $N = 65$ and $R = 1.5$.

0.0
0.0
0.0
0.0
0.0
0.0
-0.11330
-0.24668
-0.22178
-0.15401
-0.06501
0.03315
0.13436
0.23487
0.33357
0.42932
0.51350
0.60518
0.68603
0.76181
0.83172
0.89571
0.95546
1.00798
1.05503
1.09827
1.13429
1.16478
1.18974
1.21074
1.22461
1.23293
1.23570
1.23293
1.22461
1.21074
1.18974
1.16478
1.13429
1.09827
1.05503
1.00798

APPENDIX G. COMPARISON OF JONES1 AND JONES2 VALUES OF THE INSIDE INTEGRAL WITH VAN HOUTEN'S VALUES OF THE INSIDE INTEGRAL

| R | VALUE OF INSIDE INTEGRAL | | % DIFFERENCE BETWEEN JONES1 AND VAN HOUTEN'S | |
|----------|--------------------------|----------|--|------------|
| | VAN HOUTEN'S | JONES1 | JONES2 | |
| -1.50000 | 0.69758 | 0.69181 | 0.69179 | 1 0.83 |
| -1.45313 | 0.66847 | 0.67833 | 0.67839 | 2 -1.48 |
| -1.40625 | 0.66746 | 0.60559 | 0.60561 | 3 -9.27 |
| -1.35938 | 0.37190 | 0.37536 | 0.37535 | 4 -0.93 |
| -1.31250 | 0.02912 | 0.44074 | -0.44074 | 5 -1413.53 |
| -1.26563 | -0.41609 | -0.29548 | -0.29548 | 6 91.35 |
| -1.21875 | 2.84182 | 3.64357 | 3.64358 | 7 -28.21 |
| -1.17183 | 12.47668 | 8.13610 | 8.13610 | 8 34.77 |
| -1.12500 | 8.91488 | 8.48982 | 8.48580 | 9 4.77 |
| -1.07813 | 6.96253 | 6.58171 | 6.58170 | 10 5.47 |
| -1.03125 | 4.88435 | 4.85099 | 4.85099 | 11 0.68 |
| -1.08438 | 3.38097 | 3.35730 | 3.35730 | 12 0.70 |
| -0.93750 | 2.05348 | 2.10854 | 2.10849 | 13 -2.68 |
| -0.89063 | 1.01299 | 1.06492 | 1.06489 | 14 -5.13 |
| -0.84375 | 0.10356 | 0.16184 | 0.16183 | 15 -56.23 |
| -0.79688 | -0.75777 | -0.61879 | -0.61880 | 16 16.18 |
| -0.75000 | -1.34876 | -1.26543 | -1.26546 | 17 6.36 |
| -0.70313 | -1.90174 | -1.81883 | -1.81888 | 18 4.33 |
| -0.65625 | -2.40410 | -2.31692 | -2.31693 | 19 3.69 |
| -0.60938 | -2.86302 | -2.75728 | -2.75726 | 20 3.41 |
| -0.56250 | -3.23576 | -3.12539 | -3.12540 | 21 1.72 |
| -0.51563 | -3.49790 | -3.44993 | -3.44995 | 22 3.82 |
| -0.46875 | -3.89733 | -3.74847 | -3.74853 | 23 2.89 |
| -0.42188 | -4.06769 | -3.97713 | -3.97713 | 24 3.30 |
| -0.37500 | -4.21588 | -4.17841 | -4.17841 | 25 1.79 |
| -0.32813 | -4.53605 | -4.38655 | -4.38660 | 26 2.15 |
| -0.28125 | -4.62380 | -4.54113 | -4.54122 | 27 2.83 |
| -0.23438 | -4.74552 | -4.64331 | -4.64341 | 28 2.08 |
| -0.18750 | -4.78919 | -4.74920 | -4.74930 | 29 1.70 |
| -0.14063 | -5.00409 | -4.85953 | -4.85956 | 30 1.88 |
| -0.09375 | -5.00427 | -4.92306 | -4.92316 | 31 1.78 |
| -0.04688 | -5.04047 | -4.94558 | -4.94558 | 32 1.88 |
| 0.00000 | -5.04047 | -4.94553 | -4.94565 | 33 1.70 |
| 0.04688 | -5.00042 | -4.85958 | -4.85969 | 34 2.89 |
| 0.09375 | -5.00040 | -4.85955 | -4.85966 | 35 2.89 |
| 0.14063 | -5.00040 | -4.85955 | -4.85966 | 36 2.89 |

0.8 16
 0.2 1.3 0
 1.3 0.2 2.8 3.2 7.1 0.3 6.3 6.8
 1.3 3.3 4.6 1.4 8.3 8
 16.5 1.4 8.3 8
 -5.5 1.6 8.3 8
 -2.0 0.6 8.3 8
 5.4 7.7 9
 34.7 7.9
 -28.2 1.5 0
 -91.3 5.0 3.7 8.3
 -141.3 0.2 2.4 8.3
 -9.1 4.8
 -1.0

37 38 39 40 41 42 43 44 45 46 47 48 49 50 51 52 53 54 55 56 57 58 59 60 61 62 63 64 65

74 93 1
 -4.6 43 40
 -4.5 41 20
 -4.3 86 57
 -4.3 178 42
 -3.5 77 14
 -3.7 48 59
 -3.4 49 99
 -3.1 25 35
 -2.7 57 25
 -2.3 16 54
 -1.8 18 43
 -1.2 61 82
 -0.1 64 50
 1.0 85 22
 2.3 57 31
 4.6 50 98
 6.8 58 167
 8.3 48 97 89
 3.6 36 09
 -0.2 95 58
 -0.3 54 8
 0.3 29 54 8
 0.3 74 4
 0.3 75 55
 0.6 78 38
 0.6 91 81

74 91 7
 -4.6 43 22
 -4.5 41 06
 -4.3 86 56
 -4.3 178 40
 -3.5 77 06
 -3.7 48 45
 -3.4 49 35
 -3.1 25 35
 -2.7 57 19
 -2.3 16 89
 -1.8 18 87
 -1.2 61 82
 -0.1 64 53
 1.0 85 43
 2.3 57 32
 4.6 50 99
 6.8 58 171
 8.3 48 97 50
 3.6 36 00
 -0.2 95 50
 -0.3 54 73
 0.3 29 53 7
 0.3 74 59
 0.3 75 55
 0.6 78 35
 0.6 91 79

74 91 9
 -4.6 43 52
 -4.5 41 38
 -4.3 86 05
 -4.3 178 58
 -3.5 77 69
 -3.7 48 33
 -3.4 49 79
 -3.1 25 30
 -2.7 57 62
 -2.3 16 40
 -1.8 18 74
 -1.2 61 76
 -0.1 64 77
 1.0 85 33
 2.3 57 56
 4.6 50 99
 6.8 58 47
 8.3 48 35
 3.6 36 25
 -0.2 95 38
 -0.3 54 88
 0.3 29 18
 0.3 74 82
 0.3 75 92
 0.6 78 46
 0.6 91 58

0.1 87 50
 0.2 38 12
 0.3 25 13
 0.4 28 13
 0.5 37 50
 0.6 48 18
 0.7 56 33
 0.8 65 50
 0.9 73 25
 1.0 82 30
 1.1 90 10
 1.2 96 33
 1.3 103 50
 1.4 110 63
 1.5 117 75
 1.6 124 88
 1.7 131 00
 1.8 138 13
 1.9 145 25
 2.0 152 38
 2.1 159 50
 2.2 166 63
 2.3 173 75
 2.4 180 88
 2.5 187 00
 2.6 194 13
 2.7 201 25
 2.8 208 38
 2.9 215 50
 3.0 222 63
 3.1 229 75
 3.2 236 88
 3.3 243 00
 3.4 250 13
 3.5 257 25
 3.6 264 38
 3.7 271 50
 3.8 278 63
 3.9 285 75
 4.0 292 88
 4.1 299 00
 4.2 306 13
 4.3 313 25
 4.4 320 38
 4.5 327 50
 4.6 334 63
 4.7 341 75
 4.8 348 88
 4.9 355 00
 5.0 362 13
 5.1 369 25
 5.2 376 38
 5.3 383 50
 5.4 390 63
 5.5 397 75
 5.6 404 88
 5.7 411 00
 5.8 418 13
 5.9 425 25
 6.0 432 38
 6.1 439 50
 6.2 446 63
 6.3 453 75
 6.4 460 88
 6.5 467 00
 6.6 474 13
 6.7 481 25
 6.8 488 38
 6.9 495 50
 7.0 502 63
 7.1 509 75
 7.2 516 88
 7.3 523 00
 7.4 530 13
 7.5 537 25
 7.6 544 38
 7.7 551 50
 7.8 558 63
 7.9 565 75
 8.0 572 88
 8.1 579 00
 8.2 586 13
 8.3 593 25
 8.4 600 38
 8.5 607 50
 8.6 614 63
 8.7 621 75
 8.8 628 88
 8.9 635 00
 9.0 642 13
 9.1 649 25
 9.2 656 38
 9.3 663 50
 9.4 670 63
 9.5 677 75
 9.6 684 88
 9.7 691 00
 9.8 698 13
 9.9 705 25
 10.0 712 38
 10.1 719 50
 10.2 726 63
 10.3 733 75
 10.4 740 88
 10.5 747 00
 10.6 754 13
 10.7 761 25
 10.8 768 38
 10.9 775 50
 11.0 782 63
 11.1 789 75
 11.2 796 88
 11.3 803 00
 11.4 810 13
 11.5 817 25
 11.6 824 38
 11.7 831 50
 11.8 838 63
 11.9 845 75
 12.0 852 88
 12.1 859 00
 12.2 866 13
 12.3 873 25
 12.4 880 38
 12.5 887 50
 12.6 894 63
 12.7 901 75
 12.8 908 88
 12.9 915 00
 13.0 922 13
 13.1 929 25
 13.2 936 38
 13.3 943 50
 13.4 950 63
 13.5 957 75
 13.6 964 88
 13.7 971 00
 13.8 978 13
 13.9 985 25
 14.0 992 38
 14.1 999 50
 14.2 1006 63
 14.3 1013 75
 14.4 1020 88
 14.5 1027 00
 14.6 1034 13
 14.7 1041 25
 14.8 1048 38
 14.9 1055 50
 15.0 1062 63
 15.1 1069 75
 15.2 1076 88
 15.3 1083 00
 15.4 1090 13
 15.5 1097 25
 15.6 1104 38
 15.7 1111 50
 15.8 1118 63
 15.9 1125 75
 16.0 1132 88
 16.1 1139 00
 16.2 1146 13
 16.3 1153 25
 16.4 1160 38
 16.5 1167 50
 16.6 1174 63
 16.7 1181 75
 16.8 1188 88
 16.9 1195 00
 17.0 1202 13
 17.1 1209 25
 17.2 1216 38
 17.3 1223 50
 17.4 1230 63
 17.5 1237 75
 17.6 1244 88
 17.7 1251 00
 17.8 1258 13
 17.9 1265 25
 18.0 1272 38
 18.1 1279 50
 18.2 1286 63
 18.3 1293 75
 18.4 1300 88
 18.5 1307 00
 18.6 1314 13
 18.7 1321 25
 18.8 1328 38
 18.9 1335 50
 19.0 1342 63
 19.1 1349 75
 19.2 1356 88
 19.3 1363 00
 19.4 1370 13
 19.5 1377 25
 19.6 1384 38
 19.7 1391 50
 19.8 1398 63
 19.9 1405 75
 20.0 1412 88
 20.1 1419 00
 20.2 1426 13
 20.3 1433 25
 20.4 1440 38
 20.5 1447 50
 20.6 1454 63
 20.7 1461 75
 20.8 1468 88
 20.9 1475 00
 21.0 1482 13
 21.1 1489 25
 21.2 1496 38
 21.3 1503 50
 21.4 1510 63
 21.5 1517 75
 21.6 1524 88
 21.7 1531 00
 21.8 1538 13
 21.9 1545 25
 22.0 1552 38
 22.1 1559 50
 22.2 1566 63
 22.3 1573 75
 22.4 1580 88
 22.5 1587 00
 22.6 1594 13
 22.7 1601 25
 22.8 1608 38
 22.9 1615 50
 23.0 1622 63
 23.1 1629 75
 23.2 1636 88
 23.3 1643 00
 23.4 1650 13
 23.5 1657 25
 23.6 1664 38
 23.7 1671 50
 23.8 1678 63
 23.9 1685 75
 24.0 1692 88
 24.1 1699 00
 24.2 1706 13
 24.3 1713 25
 24.4 1720 38
 24.5 1727 50
 24.6 1734 63
 24.7 1741 75
 24.8 1748 88
 24.9 1755 00
 25.0 1762 13
 25.1 1769 25
 25.2 1776 38
 25.3 1783 50
 25.4 1790 63
 25.5 1797 75
 25.6 1804 88
 25.7 1811 00
 25.8 1818 13
 25.9 1825 25
 26.0 1832 38
 26.1 1839 50
 26.2 1846 63
 26.3 1853 75
 26.4 1860 88
 26.5 1867 00
 26.6 1874 13
 26.7 1881 25
 26.8 1888 38
 26.9 1895 50
 27.0 1902 63
 27.1 1909 75
 27.2 1916 88
 27.3 1923 00
 27.4 1930 13
 27.5 1937 25
 27.6 1944 38
 27.7 1951 50
 27.8 1958 63
 27.9 1965 75
 28.0 1972 88
 28.1 1979 00
 28.2 1986 13
 28.3 1993 25
 28.4 2000 38
 28.5 2007 50
 28.6 2014 63
 28.7 2021 75
 28.8 2028 88
 28.9 2035 00
 29.0 2042 13
 29.1 2049 25
 29.2 2056 38
 29.3 2063 50
 29.4 2070 63
 29.5 2077 75
 29.6 2084 88
 29.7 2091 00
 29.8 2098 13
 29.9 2105 25
 30.0 2112 38
 30.1 2119 50
 30.2 2126 63
 30.3 2133 75
 30.4 2140 88
 30.5 2147 00
 30.6 2154 13
 30.7 2161 25
 30.8 2168 38
 30.9 2175 50
 31.0 2182 63
 31.1 2189 75
 31.2 2196 88
 31.3 2203 00
 31.4 2210 13
 31.5 2217 25
 31.6 2224 38
 31.7 2231 50
 31.8 2238 63
 31.9 2245 75
 32.0 2252 88
 32.1 2259 00
 32.2 2266 13
 32.3 2273 25
 32.4 2280 38
 32.5 2287 50
 32.6 2294 63
 32.7 2301 75
 32.8 2308 88
 32.9 2315 00
 33.0 2322 13
 33.1 2329 25
 33.2 2336 38
 33.3 2343 50
 33.4 2350 63
 33.5 2357 75
 33.6 2364 88
 33.7 2371 00
 33.8 2378 13
 33.9 2385 25
 34.0 2392 38
 34.1 2399 50
 34.2 2406 63
 34.3 2413 75
 34.4 2420 88
 34.5 2427 00
 34.6 2434 13
 34.7 2441 25
 34.8 2448 38
 34.9 2455 50
 35.0 2462 63
 35.1 2469 75
 35.2 2476 88
 35.3 2483 00
 35.4 2490 13
 35.5 2497 25
 35.6 2504 38
 35.7 2511 50
 35.8 2518 63
 35.9 2525 75
 36.0 2532 88
 36.1 2539 00
 36.2 2546 13
 36.3 2553 25
 36.4 2560 38
 36.5 2567 50
 36.6 2574 63
 36.7 2581 75
 36.8 2588 88
 36.9 2595 00
 37.0 2602 13
 37.1 2609 25
 37.2 2616 38
 37.3 2623 50
 37.4 2630 63
 37.5 2637 75
 37.6 2644 88
 37.7 2651 00
 37.8 2658 13
 37.9 2665 25
 38.0 2672 38
 38.1 2679 50
 38.2 2686 63
 38.3 2693 75
 38.4 2700 88
 38.5 2707 00
 38.6 2714 13
 38.7 2721 25
 38.8 2728 38
 38.9 2735 50
 39.0 2742 63
 39.1 2749 75
 39.2 2756 88
 39.3 2763 00
 39.4 2770 13
 39.5 2777 25
 39.6 2784 38
 39.7 2791 50
 39.8 2798 63
 39.9 2805 75
 40.0 2812 88
 40.1 2819 00
 40.2 2826 13
 40.3 2833 25
 40.4 2840 38
 40.5 2847 50
 40.6 2854 63
 40.7 2861 75
 40.8 2868 88
 40.9 2875 00
 41.0 2882 13
 41.1 2889 25
 41.2 2896 38
 41.3 2903 50
 41.4 2910 63
 41.5 2917 75
 41.6 2924 88
 41.7 2931 00
 41.8 2938 13
 41.9 2945 25
 42.0 2952 38
 42.1 2959 50
 42.2 2966 63
 42.3 2973 75
 42.4 2980 88
 42.5 2987 00
 42.6 2994 13
 42.7 3001 25
 42.8 3008 38
 42.9 3015 50
 43.0 3022 63
 43.1 3029 75
 43.2 3036 88
 43.3 3043 00
 43.4 3050 13
 43.5 3057 25
 43.6 3064 38
 43.7 3071 50
 43.8 3078 63
 43.9 3085 75
 44.0 3092 88
 44.1 3099 00
 44.2 3106 13
 44.3 3113 25
 44.4 3120 38
 44.5 3127 50
 44.6 3134 63
 44.7 3141 75
 44.8 3148 88
 44.9 3155 00
 45.0 3162 13
 45.1 3169 25
 45.2 3176 38
 45.3 3183 50
 45.4 3190 63
 45.5 3197 75
 45.6 3204 88
 45.7 3211 00
 45.8 3218 13
 45.9 3225 25
 46.0 3232 38
 46.1 3239 50
 46.2 3246 63
 46.3 3253 75
 46.4 3260 88
 46.5 3267 00
 46.6 3274 13
 46.7 3281 25
 46.8 3288 38
 46.9 3295 50
 47.0 3302 63
 47.1 3309 75
 47.2 3316 88
 47.3 3323 00
 47.4 3330 13
 47.5 3337 25
 47.6 3344 38
 47.7 3351 50
 47.8 3358 63
 47.9 3365 75
 48.0 3372 88
 48.1 3379 00
 48.2 3386 13
 48.3 3393 25
 48.4 3400 38
 48.5 3407 50
 48.6 3414 63
 48.7 3421 75
 48.8 3428 88
 48.9 3435 00
 49.0 3442 13
 49.1 3449 25
 49.2 3456 38
 49.3 3463 50
 49.4 3470 63
 49.5 3477 75
 49.6 3484 88
 49.7 3491 00
 49.8 3498 13
 49.9 3505 25
 50.0 3512 38
 50.1 3519 50
 50.2 3526 63
 50.3 3533 75
 50.4 3540 88
 50.5 3547 00
 50.6 3554 13
 50.7 3561 25
 50.8 3568 38
 50.9 3575 50
 51.0 3582 63
 51.1 3589 75
 51.2 3596 88
 51.3 3603 00
 51.4 3610 13
 51.5 3617 25
 51.6 3624 38
 51.7 3631 50
 51.8 3638 63
 51.9 3645 75
 52.0 3652 88
 52.1 3659 00
 52.2 3666 13
 52.3 3673 25
 52.4 3680 38
 52.5 3687 50
 52.6 3694 63
 52.7 3701 75
 52.8 3708 88
 52.9 3715 00
 53.0 3722 13
 53.1 3729 25
 53.2 3736 38
 53.3 3743 50
 53.4 3750 63
 53.5 3757 75
 53.6 3764 88
 53.7 3771 00
 53.8 3778 13
 53.9 3785 25
 54.0 3792 38
 54.1 3799 50
 54.2 3806 63
 54.3 3813 75
 54.4 3820 88
 54.5 3827 00
 54.6 3834 13
 54.7 3841 25
 54.8 3848 38
 54.9 3855 50
 55.0 3862 63
 55.1 3869 75
 55.2 3876 88
 55.3 3883 00
 55.4 3890 13
 55.5 3897 25
 55.6 3904 38
 55.7 3911 50
 55.8 3918 63
 55.9 3925 75
 56.0 3932 88
 56.1 3939 00
 56.2 3946 13
 56.3 3953 25
 56.4 3960 38
 56.5 3967 50
 56.6 3974 63
 56.7 3981 75
 56.8 3988 88
 56.9 3995 00
 57.0 4002 13
 57.1 4009 25
 57.2 4016 38
 57.3 4023 50
 57.4 4030 63
 57.5 4037 75
 57.6 4044 88
 57.7 4051 00
 57.8 4058 13
 57.9 4065 25
 58.0 4072 38
 58.1 4079 50
 58.2 4086 63
 58.3 4093 75
 58.4 4100 88
 58.5 4107 00
 58.6 4114 13
 58.7 4121 25
 58.8 4128 38
 58.9 4135 50
 59.0 4142 63
 59.1 4149 75
 59.2 4156 88
 59.3 4163 00
 59.4 4170 13
 59.5 4177 25
 59.6 4184 38
 59.7 4191 50
 59.8 4198 63
 59.9 4205 75
 60.0 4212 88
 60.1 4219 00
 60.2 4226 13
 60.3 4233 25
 60.4 4240 38
 60.5 4247 50
 60.6 4254 63
 60.7 4261 75
 60.8 4268 88
 60.9 4275 00
 61.0 4282 13
 61.1 4289 25
 61.2 4296 38
 61.3 4303 50
 61.4 4310 63
 61.5 4317 75
 61.6 4324 88
 61.7 4331 00
 61.8 4338 13
 61.9 4345 25
 62.0 4352 38
 62.1 4359 50
 62.2 4366 63
 62.3 4373 75
 62.4 4380 88
 62.5 4387 00
 62.6 4394 13
 62.7 4401 25
 62.8 4408 38
 62.9 4415 50
 63.0 4422 63
 63.1 4429 75
 63.2 4436 88
 63.3 4443 00
 63.4 4450 13
 63.5 4457 25
 63.6 4464 38
 63.7 4471 50
 63.8 4478 63
 63.9 4485 75
 64.0 4492 88
 64.1 4499 00
 64.2 4506 13
 64.3 4513 25
 64.4 4520 38

REFERENCES

1. Gabor, D., "A New Microscopic Principle," Nature 161, 777, 1948.
2. Gabor, D., "Microscopy by Reconstructed Wavefronts," Proceedings of the Royal Society A 197, 454, 1949.
3. Collier, R., Burckhardt, C.B., and Lin, L.H., Optical Holography, Academic Press, New York, 1971.
4. Collins, D., "Measurement of Velocities in Single and Two-Phase Flows," von Karmen Institute for Fluid Dynamics, Lecture Series 54, 19-23 February, 1973.
5. Radley, R.J., Jr. and Havener, A.G., "The Application of Dual Hologram Interferometry to Wind Tunnel Testing," AIAA Paper 73-210, Washington, D.C., 1973.
6. Chapman, D.R., Kuehn, D.M., and Larson, H.K., "Investigation of Separated Flows in Supersonic and Subsonic Streams with Emphasis on the Effect of Transition," NACA TN 3869, 1957.
7. Korst, H.H., "A Theory for Base Pressures in Transonic and Supersonic Flow," ASME Journal of App. Mech. 23, 593-600, 1956.
8. Roache, P.J., "Numerical Solutions of Compressible and Incompressible Laminar Separated Flows," Ph.D. Thesis, University of Notre Dame, 1968, University Microfilms, Inc., Ann Arbor, Michigan, 1970.
9. Wazzan, A.R., "Review of Recent Developments in Turbulent Supersonic Base Flow," AIAA Journal 3, 1135, 1965.
10. Schlichting, H., Boundary Layer Theory, 6th ed., 26,41, McGraw-Hill Book Co., New York, N.Y., 1968.
11. Nassenstein, H., et al, Engineering Uses of Holography, 25, Cambridge University Press, 1970.
12. Sweeney, D.W., "Interferometric Measurement of Three-Dimensional Temperature Fields," Ph.D. Thesis, University of Michigan, 1972.
13. Matulka, R.D., "The Application of Holographic Interferometry to the Determination of Asymmetric Three-Dimensional Density Field in Free Jet Flow," Ph.D. Thesis, Naval Postgraduate School, Monterey, Ca., 1970.
14. Rowley, P., "Quantitative Interpretation of Three-Dimensional Weakly Refractive Phase Objects Using Holographic Interferometry," Journal of the American Optical Society 59, 1496, 1969.

15. Junginger, H.G. and van Haeringer, W., "Calculation of Three-Dimensional Refractive Index Field using Phase Integrals," Optics Communications 5, 1, 1972.
16. Sweeney, D.W., "Interferometric Measurement of Three-Dimensional Temperature Fields," Ph.D. Thesis, University of Michigan, 1972.
17. Van Houten, P., "The Application of Holographic Interferometry to the Determination of Discontinuous Three-Dimensional Density Fields," A. E. Thesis, Naval Postgraduate School, Monterey, Ca., 1972.
18. Froberg, C., Introduction to Numerical Analysis, 195-223, Addison-Wesley Publishing Co., 1965.
19. Bergland, G.D., "A Guided Tour of the Fast Fourier Transform," Bell Telephone Laboratories, Inc., IEEE Spectrum, July, 1969.
20. Brigham, E.O., The Fast Fourier Transform, 198-221, Prentice-Hall, Inc., Englewood Cliffs, New Jersey, 1974.
21. Everett, R., "Experimental Techniques in Holographic Interferometry," Naval Postgraduate School, Monterey, Ca., 1973.
22. Singleton, R.C., "An Algorithm for Computing the Mixed Radix Fast Fourier Transform," IEEE Transactions on Audio and Electroacoustics AU17-2, June, 1969.

INITIAL DISTRIBUTION LIST

| | No. Copies |
|--|------------|
| 1. Defense Documentation Center Cameron Station Alexandria, Virginia 22314 | 2 |
| 2. Library (Code 0212) Naval Postgraduate School Monterey, California 93940 | 2 |
| 3. Chairman Department of Aeronautics Code 57 Naval Postgraduate School Monterey, California 93940 | 1 |
| 4. Professor D.J. Collins Department of Aeronautics Code 57C0 Naval Postgraduate School Monterey, California 93940 | 2 |
| 5. LT Harland W. Jones, Jr., USN Air Department USS America CVA-66 FPO New York, New York | 1 |

| REPORT DOCUMENTATION PAGE | | READ INSTRUCTIONS BEFORE COMPLETING FORM |
|---|-----------------------|--|
| 1. REPORT NUMBER | 2. GOVT ACCESSION NO. | 3. RECIPIENT'S CATALOG NUMBER |
| 4. TITLE (and Subtitle) Application of Holographic Interferometry to a Supersonic Flow Visualization of a Rear-Facing Step and Application of Fast Fourier Transform Methods to Current Data Reduction Techniques | | 5. TYPE OF REPORT & PERIOD COVERED Master's Thesis; March 1974 |
| | | 6. PERFORMING ORG. REPORT NUMBER |
| 7. AUTHOR(s) Harland Wilber Jones, Jr. | | 8. CONTRACT OR GRANT NUMBER(s) |
| 9. PERFORMING ORGANIZATION NAME AND ADDRESS Naval Postgraduate School Monterey, California 93940 | | 10. PROGRAM ELEMENT, PROJECT, TASK AREA & WORK UNIT NUMBERS |
| 11. CONTROLLING OFFICE NAME AND ADDRESS Naval Postgraduate School Monterey, California 93940 | | 12. REPORT DATE March 1974 |
| | | 13. NUMBER OF PAGES 90 |
| 14. MONITORING AGENCY NAME & ADDRESS (if different from Controlling Office) Naval Postgraduate School Monterey, California 93940 | | 15. SECURITY CLASS. (of this report) Unclassified |
| | | 15a. DECLASSIFICATION/DOWNGRADING SCHEDULE |
| 16. DISTRIBUTION STATEMENT (of this Report) Approved for public release; distribution unlimited. | | |
| 17. DISTRIBUTION STATEMENT (of the abstract entered in Block 20, if different from Report) | | |
| 18. SUPPLEMENTARY NOTES | | |
| 19. KEY WORDS (Continue on reverse side if necessary and identify by block number) Holographic Interferometry Fast Fourier Transform Interferometric Measurement Supersonic Flow Visualization Rear-Facing Step Flow | | |
| 20. ABSTRACT (Continue on reverse side if necessary and identify by block number) The successful application of holographic interferometry to the study of three-dimensional density fields around bodies in wind tunnel experiments has been reported in the literature along with the associated mathematical reduction processes for the basic interferometric equation. The present report has extended the application of holography as a flow visualization technique by investigating Mach 2.8 flow over a rear-facing 1/8 in. step. Two single-exposed holograms of the model and two double- | | |

20. (cont'd)

exposed frozen fringe holographic interferograms of the flow were created.

Fast Fourier Transform (FFT) methods have been reported as significantly reducing computational time to obtain discrete and inverse discrete Fourier transforms. Two computer programs were designed to apply FFT methods to the Fourier transform approach to the basic interferometric equation. These programs were used to investigate an alternate way to calculate the value of the inside integral. Total agreement was not found, and further analysis as to the accuracy of each method is needed.

20970

Thesis

150868

J7195

Jones

c.1

Application of holographic interferometry to supersonic flow visualization of a rear-facing step and application of fast fourier transform methods to current data reduction techniques.

Th
J
c

20970

Thesis

150868

J7195

Jones

c.1

Application of holographic interferometry to supersonic flow visualization of a rear-facing step and application of fast fourier transform methods to current data reduction techniques.

thesJ7195

Application of holographic interferometr



3 2768 002 10589 2

DUDLEY KNOX LIBRARY